

2

LIBRARY
Michigan State
University



This is to certify that the

thesis entitled

Laser Die-Less Forming of Superplastic

Materials

presented by

Ning Hu

has been accepted towards fulfillment of the requirements for

Master's degree in Materials Science

Date July 2, 1998

MSU is an Affirmative Action/Equal Opportunity Institution

Kali mukherje.

Major professor

PLACE IN RETURN BOX to remove this checkout from your record.

TO AVOID FINES return on or before date due.

MAY BE RECALLED with earlier due date if requested.

DATE DUE	DATE DUE	DATE DUE

1/98 c:/CIRC/DateDue.p65-p.14

LASER DIE-LESS FORMING OF SUPERPLASTIC MATERIALS

By

Ning Hu

A THESIS

Submitted to

Michigan State University

In partial fulfillment of the requirements

for the degree of

MASTER OF SCIENCE

Department of Materials Science and Mechanics

1998

ABSTRACT

LASER DIE-LESS FORMING OF SUPERPLASTIC MATERIALS

By

Ning Hu

Traditional forming of a "superplastic" sheet can be accomplished by using a gas pressure to blow, or using vacuum to draw the sheet into a die cavity, when the temperature of the sheet reaches the superplastic deformation temperature.

An innovative study on the feasibility of using high energy laser to deform plastic and superplastic materials was conducted in the High Energy Laser Materials Processing Laboratory HELP of Michigan State University. This novel superplastic sheet forming technique is vastly different from the conventional superplastic forming process. In this study, a high energy CO₂ laser was controlled to perform heating, at selected and programmed locations, on a superplastic sheet which is situated on a box containing a gas at higher than ambient pressure, or vacuum. Both the geometry of the heating path and the amount of heat input could be precisely implemented through computer numerical control (CNC). Convex or concave bulges, which will delineate a desired shape, can be obtained.

With the experimental results, the feasibility of laser die-less superplastic forming has successfully demonstrated the economic and practical potential in complex shape forming. It is even possible to control not only the final thickness, but also the deformed shape by using this technique. Since the quality of the workpiece can be controlled at any region of processing without the use of a die, a complex fabrication seems possible.

DEDICATION

To my parents and my husband:

for their understanding, encouragement, and support

ACKNOWLEDGEMENTS

I want to express my sincere appreciation and gratitude to Prof. K. Mukherjee, my advisor, for his guidance, encouragement, and financial support throughout the period of this study. I also would like to thank Prof. T.R.Bieler, who provided a lot of valuable advice and theoretical instruction for my research. Special thanks to Prof. J. P. Lucas and Prof. P. Y. Kwon for their invaluable suggestions for improving this thesis.

Sincere gratitude is extended to Dr. C.W.Chen, for his specific technical assistance and patient help. Helpful suggestions received from Mr. Yiping Hu, and Mr. J. K. Park are gratefully acknowledged.

TABLE OF CONTENTS

LIST OF	F TABLES	viii
LIST OF	F FIGURES	ix
1 INTRO	OF FIGURES ix RODUCTION 1 ERPLASTICITY & SUPERPLASTIC FORMING History of Superplasticity 4 Properties of Superplastic Materials 5 Theory of Superplasticity 6 Requirement for Superplastic Materials 10 Superplastic Forming Techniques 10 INCIPLE OF LASER & LASER MATERIALS PROCESSING Principle of Laser Operation 15 3.1.1 Radiation of Light Quantum 15 3.1.2 Stimulated Emission 16 CO2 Laser 20 The Characteristic of Laser Beam 22 3.3.1 The Property of Continuos Beam 22 3.3.2 The "Mode" of Laser Beam with Materials 25 Laser Applications in Materials Processing 29 3.5.1 Laser Cutting 29 3.5.2 Laser Welding 30 3.5.3 Laser Surface Treatment 30 3.5.4 Laser Forming (Bending) 32 SER DIELESS SUPERPLASTIC METAL FORMING 33 The Function of Laser Beam 34 4.1.1 Laser Beam Power 34	
2 SUPER		
2.1	History of Superplasticity	4
2.2	Properties of Superplastic Materials	5
2.3	Theory of Superplasticity	6
2.4	Requirement for Superplasticity	9
2.5	Types of Superplastic Materials	10
2.6	Superplastic Forming Techniques	10
3 PRINC	CIPLE OF LASER & LASER MATERIALS PROCESS	SING
3.1	Principle of Laser Operation	15
3.1	1.1 Radiation of Light Quantum	15
3.1	1.2 Stimulated Emission	16
3.2	CO ₂ Laser	20
3.3	The Characteristic of Laser Beam	22
3.3	3.1 The Property of Continuos Beam	22
3.3	.3.2 The "Mode" of Laser Beam	23
3.4	Interaction of Laser Beam with Materials	25
3.5	Laser Applications in Materials Processing	29
3.5	.5.1 Laser Cutting	29
3.5	.5.2 Laser Welding	30
3.5	.5.3 Laser Surface Treatment	30
3.5	.5.4 Laser Forming (Bending)	32
4 LASE	ER DIELESS SUPERPLASTIC METAL FORMING	33
4.1	The Function of Laser Beam	33
4.	.1.1 Laser Beam Power	34
4.	.1.2 Laser Beam Diameter	34

	4.1.3	Beam Traverse Speed	36
	4.1.4	Beam Scanning Track	37
	4.2 F	Forming Force	37
5	EXPERI	MENTAL PROCEDURE	39
	5.1 I	Experimental Setup	39
	5.1.1	CO ₂ Laser	39
	5.1.2	CAM System.	42
	5.1.3	Superplastic Forming System	43
	5.1.4	Measurement System	45
	5.2	Preparation of Testing Materials	45
	5.3	General Description of Experiments	48
6	RESULT	'S AND DISCUSSION	50
	6.1	Investigation of Laser Energy Effect	50
	6.1.1	The Influence of the Laser Parameters	50
	6.1	.1.1 Small Beam Diameter at Different Traverse Speed	51
	6.1	1.1.2 Large Beam Diameter	54
	6.2	Measurement of Temperature Distribution	56
	6.2.1	Two Points Measurement (dynamic state)	60
	6.2.2	Center Point Measurement (static state)	64
	6.2.3	Four Points Measurement (static state)	66
	6.3	Evaluation of Microstructure	74
	6.3.1	Grain Growth at Furnace Heat Treatment	74
	6.3.2	Grain Growth during Laser Process Heating	80
	6.4	Measurement of Strain and Strain Rate	80
	6.5	The Variation of the Thickness	85
7	SUMMI	ERY	91
R	IRI AIGE	PAPHV	03

LIST OF TABLES

1.	Superplastic properties of several alloys	11
2.	The Characteristics of RF excited CO ₂ laser	42
3.	Specifications of the CNC machine	43
4.	Composition and selected mechanical properties of GK 45 alloy	48
5.	The parameters used in the experiment for testing energy absorption	52

LIST OF FIGURES

1.	The relationship between stress and strain rate
2.	The relationship between strain rate sensitivity exponent, m, and strain rate7
3.	A schematic view of sequence for superplastic forming process12
4.	Spontaneous photon emission
5 .	Photon stimulated transition of an electron and photon emission17
6.	Balance of absorption and emission in steady state:
	(a) stimulated emission; (b) absorption; (c) spontaneous emission18
7.	A vibration mode of CO ₂ atoms21
8.	Energy levels of CO ₂ laser
9.	Transverse-mode patterns in rectangular and cylindrical symmetry24
10.	Surface temperature of Al as a function of time for various absorbed energy.
	The dotted line shows the shape of the Gaussian laser beam mode.
	Melt depth as a function of time with velocity of the liquid-solid interface 27
11.	Reflectivity as a function of wavelength for several metals
12.	Schematic diagram of CNC laser assisted superplastic forming35
13.	Schematic diagram showing the vacuum chamber used in conjunction
	with laser process
14.	A photograph showing the laser nozzle, chamber and temperature
	measurement setup41
15	a. A schematic diagram showing the condition of vacuum forming44
151	b. A schematic diagram showing the condition of argon gas forming44

16.	A schematic diagram showing the setup for temperature measurement45
17.	A schematic diagram showing the laser spot diameter, locus of the spot
	for generating a dome
18.	A Photograph of six patterns showing the surface condition of laser
	energy absorption by using small laser beam diameter and with
	different traverse speed. Testing material was 7475 aluminum alloy53
19.	A photograph of a sample showing the surface condition of laser
	energy absorption with a circle pattern in 7475 aluminum alloy55
20.	The temperature variation with 20mm laser spot diameter, at 350 w
	power output, traverse speed 0.42 mm/s57
21.	The temperature variation with 20mm laser spot diameter, at 470 w
	power output, traverse speed 0.42 mm/s58
22.	The temperature variation with 20mm laser spot diameter, at 470 w
	power output, traverse speed 0.105 mm/s59
23.	Two points measurement. 230 w power output and 21.16 mm/s
	traverse speed at 5 mm spot diameter61
24.	Two points measurement. 230 w power output and 8.47 mm/s
	traverse speed at 5 mm spot diameter62
25.	Two points measurement. 230 w power output and 4.23 mm/s
	traverse speed at 5 mm spot diameter63
26.	One point measurement. 345-370 w power output and 20mm

	spot diameter at static state64
27.	One point measurement. 470-490 w power output and 20mm
	spot diameter at static state65
28.	One point measurement. 570 w power output and 20mm
	spot diameter at static state65
29.	Four points measurement. Power output is 490 w
30.	Four points measurement. Power output is 550 w
31.	Temperature distribution at 70 seconds, cover gas 0.5 scfh69
32.	Temperature distribution at 70 seconds, cover gas 3.0 scfh69
33.	Temperature distribution at 350 w power output71
34.	Temperature distribution at 490 w power output72
35.	Temperature distribution at 530 w power output
36.	A photograph showing the grain size at 450°C, 40 minutes furnace annealing75
37.	A photograph showing the grain size at 500°C, 40 minutes furnace annealing76
38.	A photograph showing the grain size at 550°C, 40 minutes furnace annealing 77
39.	A photograph showing the original grain size of GK 45 alloy78
40.	The curve showing the grain size growth tendency at 40 minutes
	furnace heating condition79
41.	A photograph showing the grain size at the bottom of a deformed
	dome in GK 45 sample81
42.	A set of deformation profiles, taken at 20 minutes interval
	during the processing82

43.	The length elongation of the cross section with process time82
44.	A sketch of the cross section showing the thickness variance
	with vacuum forming system86
45.	A sketch of the cross section showing the thickness variance
	with argon gas forming system86
46.	A photograph showing the cross section appearance forming
	by vacuum
47.	A photograph showing the cross section appearance forming
	by argon gas88
48.	A sketch of showing the deformation process by a laser beam
	scanning around a circle and stable irradiation at the center87
49.	A photograph of a dome produced by LSF in GK 45 alloy. A square-mesh
	grid pattern is projected on the sample to help visualize the curvature90

Chapter 1

INTRODUCTION

In the current superplastic sheet forming industry, all products are fabricated by compressing between two matching tooling dies to obtain a desired shape. Superplastic forming has been considered as a mature processing technique for many years. This is evident by the large amount of technical literature related to superplasticity and superplastic forming.

However, the conventional methods for making both male and female dies are always time-consuming and expensive, especially for prototyping or small batch production. One reason is that the high cost of materials and labor in making die. Furthermore, the product cycle is dominated by the time spent on die making. Another reason is that the parts loading and unloading are complicated by heated forming dies, removing a formed part involves a cooling down period.

There is also a problem with the cost of the large-scale superplastic production. Further, the situation of clamping load and thermal stresses, encountered during heat-up and cooldown, can cause permanent distortions in tooling dies, so the tooling die needs to be frequently replaced. Based on the features of conventional superplastic forming process, it would be desirable if at least prototypes could be produced without need of the tooling die. This would increase the speed of marketing.

Recently, the laser materials processing techniques are being developed for numerous industrial applications. The processing that combines superplastic forming and laser processing techniques was developed to overcome the shortcomings brought by the conventional processing techniques. In this technique, plastic deformation of a superplastic metal and alloys can be produced with little mechanical contact, consequently, the hard tooling requirement is significantly reduced.

Through the experiments in this project, the feasibility of the laser dieless superplastic forming has been demonstrated. In this novel laser processing technique, laser energy was employed to work as a heating resource and localized deformation was generated by a slow scanning speed of a laser beam and gas pressures. With respect to the stationary laser beam, the target of the laser beam is moved by the computer numerical control table, which can be programmed in a CAD/CAM package.

Laser dieless superplastic forming, for manufacturing, is not yet sufficiently developed for a large scale production. However, it seems clearly possible to produce a variety of complex geometric shapes with this technique.

Compared with conventional superplastic forming processes, laser dieless superplastic forming has the following advantages:

- For rapid prototyping, and limited production, the cost of complicated devices and tooling die are not necessary.
- This economical processing procedure can increase the competitiveness of products.
- The deformation of a complex geometric shape, can be generated just by programming a desired pattern.
- The temperature, for getting correct deformation, can be controlled by adjusting the laser power parameters, and laser beam diameter.
- The final thickness, at any region of the final shape, can be controlled by patterning the deformation.

Chapter 2

SUPERPLASTICITY & SUPERPLASTIC FORMING

2.1 History of Superplasticity

It is often thought that superplasticity is a recently discovered phenomenon. In fact the phenomenon of the superplasticity was reported about eighty - five years ago, and the first paper on superplasticity was published in 1912, by Bengough [1].

However, the history of superplasticity could be traced back to the early Bronze period around 2200 BC in Turkey. At that time, the amount of ancient arsenic bronzes has been considered to contain up to 10 wt %, as used in early Bronze. Such alloys could be superplastic, since they were two-phase alloys with very small grain size. According to modern superplasticity theory, it may have developed the required stable, fine-grained superplastic structure, during hand forging into intricate shapes. From about 300 BC. to the late 19th Century, the composition of ancient steels, used in Damascus, have been discovered to be very similar to the ultrahigh carbon steel, used in modern time, which have typical superplastic characteristics. In Bengough's report[1], he described his discovery as a process in which " a certain special brass as if were pulled out to a fine point, just like pulling a glass would give rise to an enormous elongation". The concept of "amorphous cement" theory was discussed in a following paper by Rosenhain and Ewen [2]. The early stages for superplasticity were done in the late 1920's by Jenkins, [3]. After 1945, superplasticity became a common term in science coined by Bochvar and Sviderskaya [2]. Up to 1962, superplasticity was described as a firm concept based on the comprehensive review of Underwood[3], and the early experimental work of Backofen and Cowokers [3,4]. Recently, research on superplasticity has progressed much further. Its scientific merit in the context of fundamental flow and failure mechanism, as well as its technological significance in forming process, have been studied.

By now, it is very clear that superplasticity is a terminology used to describe the exceptional ductility that certain metals can exhibit when deformation conditions are

proper. It is also the deformation process that produces essentially the neck-free

elongation of many hundreds of percents in metallic materials deformed in tension [5,6].

Recently, it was recorded that in a certain metal alloy system, tensile elongation of thousands of percent has been produced. For instance, a superplastic elongation of 4,850 % was demonstrated in a Pb-62 wt % Sn alloy [7], and 5,550 % is demonstrated in a commercial aluminum bronze [8,9]. The current world record is about 7,7550% in the Pb-Sn system [10], and most recently an elongation record of 8000 % has been reported in the commercial aluminum bronze [11].

2.2 Properties of Superplastic Materials

As mentioned above, the basic definition of superplasticity is the capability of certain alloys and even certain ceramic materials to develop extremely high tensile elongation at elevated temperatures and under controlled deformation rates [12-16]. Thus, sometimes

it behaves as if it were a polymer or glass. Another characteristic is that the forces and stresses required to cause deformation, can be as little as ½ to 1/20th of that or the conventional alloy under the same conditions [17]. These two factors which are, high tensile elongation and low flow stress, provide the exceptional potential for superplastic deformation.

2.3 Theory of Superplasticity

It is well known that a major characteristic of a superplastic material is its strong resistance to necking deformation. The resistance of necking, which leads to a phenomenon of an extremely high tensile elongation at certain conditions is best measured by the value of the strain rate sensitivity exponent m. The term m is related to the rate of change of flow stress with strain rate. It is expressed in the following form:

$$m = \frac{\partial \ln \sigma}{\partial \ln \epsilon}$$

where σ is the flow stress and. $\stackrel{\bullet}{\mathcal{E}}$ is the strain rate.

The analytical relationship between $\ln \sigma$ and $\ln \varepsilon$ is shown in Figure 1.

From Fig.1, several important features are be recognized. First, the slope of the curve represents the strain rate sensitivity exponent m. Second, this plot reveals three distinct regions labeled as I, II and III, respectively. It is obvious that the strain rate sensitivity is maximum in the intermediate strain rate - region II, because the slope of the

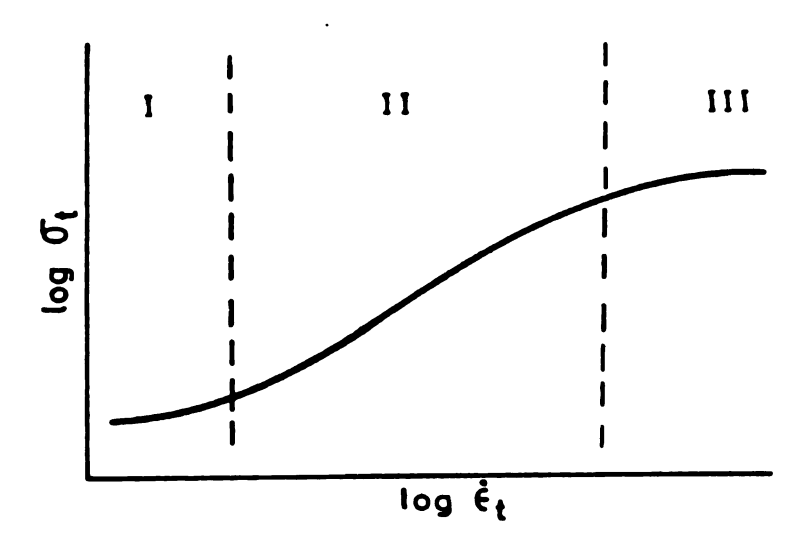


Figure 1. The relationship between stress, σ and strain rate ε [12]

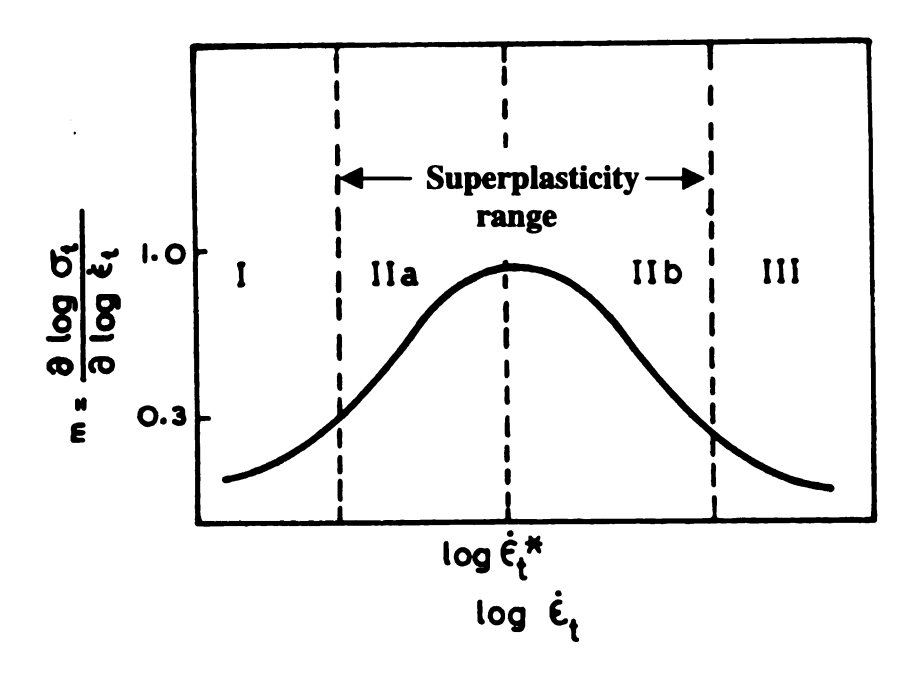


Figure 2. The relationship between strain rate sensitivity exponent, m, and strain rate $\stackrel{\bullet}{\mathcal{E}}$ [12]

curve is steeper than the slopes in the regions I and III. From the expression of the strain rate sensitivity exponent, the higher the m value, the larger the amount of stress under a certain strain rate. Therefore it indicates that the higher the m value, the stronger the resistance to necking deformation. Due to this reason, a large m value will be the desired situation for neck stability. The region II is associated with optimum superplasticity, since it is related to a grain boundary sliding mechanism. The m value of region II is equal or higher than 0.5 which meets the requirement of superplasticity. The higher strain rate located in the region III, can be correlated with dislocation creep mechanism, which is controlled by climb of edge dislocations. Usually, the m value is 0.2 or less. Up to now, the origin of the low strain rate region I, is not exactly clear because the experimental evidence in this region is often contradictory. But it is supposed that region I may be associated with Coble creep [3].

The value of m for a superplastic material is not a constant function of strain rate. The influence of variables on the strain rate sensitivity exponent, m, has been considered as strain rate, microstructure and temperature. Generally, m has a maximum value at a critical strain rate and normally the curve of m versus m looks like a bell shaped curve as shown in Figure 2. Although in some cases of superplastic deformation, m has been reported to be independent [18,19,25], and in some cases it increases [20,27] or decrease with [28,29] increasing strain rate. However, usually, it has a maximum value at a critical strain rate region [20-23]. Figure 2 shows clearly that beyond the critical strain rate or region III, and I, m decreases with strain rate at region IIb, and increases

with strain rate at region IIa. Comparing with the Figure 1, optimal superplastic deformation could be obtained in region II. On the other hand, m also increases with decreasing grain size [20,22,25] and with increasing temperature [21, 24-26].

2.4 Requirement for Superplasticity

Since there is a significant difference between normal materials and superplastic materials for ductility and tensile elongation, it is well understood that there would be some fundamental requirements for superplasticity. Studies on this objective have concluded three prime conditions for the display of superplasticity: (1) grain size must be very fine (normally less then 10 μ m), and equal-axed grain size should be stable during deformation; (2) the deformation temperature usually is higher than one half of the melting point of the matrix in Kelvin, (3) and the rate of straining must be controlled between 10^{-6} s⁻¹ and 10^{-2} s⁻¹ [3,4,17].

There are just a relatively few metals or alloys which can demonstrate superplasticity. Most metals do not maintain a fine grain size at elevated temperatures, unless the grain growth can be inhibited by some microstructural features. But the grain size also will increase when the temperature reaches more than one half the melting point, and therefore superplastic materials must be few in numbers [4,6].

2.5 Types of Superplastic Materials

Only some ferrous and nonferrous metals and alloy systems possess the potential for demonstrating superplastically. Such as titanium and aluminum alloys have a great potential for superplasticity. The application of superplastic forming techniques have been developed extensively for several materials, listed in the Table 1 [30,31].

2.6 Superplastic Forming Techniques

The term of superplastic forming means a typical process that utilizes this unique characteristic of superplasticity as illustrated in Figure 3 [5]. As shown in the schematic view, the superplastic blank is inserted between two die elements or tools, one of which is configured to the part requirement, so the lower die is the configuration die. The upper die is utilized to apply the gas pressure, to cause superplastic forming. The tooling and the superplastic blank are then placed between heated elements, which applies the heat on the superplastic blank to a suitable temperature for superplastic forming. A clamping pressure is applied to this sandwich of heated platens, and a set of tooling contains the gas pressure. The gas pressure is then imposed over the top of the sheet causing is to blow form or stretch form into the die cavity. The critical factor in superplastic forming is that the rate of applied pressure must be controlled because it reflects directly into the strain rate imposed on the superplastic blank.

Table 1. Superplastic Properties of Several Alloys [7]

Alloy	Tes temper ^o C		Strain rate s ⁻¹	Strain rate sensitivity m	Elongation %
Aluminum:					
AL-4.5Zn-4.5Ca	550	1120	8 x 10 ⁻³	0.5	600
Al-6 to 10Zn-1.5Mg-0.2Zr	550	1120	10 ⁻³	0.9	1500
Al-5.6Zn-2Mg-1.5Cu- 0.2Cr (7475)	516	961	2 x 10 ⁻⁴	0.8-0.9	800-1200
Al-6Cu-0.5Zr(Supral 100)	450	840	10 ⁻³	0.3	1000
Al-6Cu-0.35Mg-0.14Si (Supral 220)	451	840	10 ⁻³	0.3	900
Al-4Cu-3Li-0.5Zr	450	840	5 x 10 ⁻³	0.5	900
Al-3Cu-2Li-1Mg-0.2Zr	451	930	1.3 x 10 ⁻³	0.4	878
Titanium:					
Ti-6Al-4V	840-870		1.3 x 10 ⁻⁴	0.75	750-1170
Ti-6Al-5V	850	1560	5 x 10 ⁻⁴	0.70	700-1100
Ti-6Al-2Sn-4Zr-2M _O	900	1650	2 x 10 ⁻⁴	0.67	538
Ti-4.5Al-5Mo-1.5Cr	901	1600	2 x 10 ⁻⁴	0.63-0.81	>510
Ti-6Al-4V-2Ni	902	1499	2 x 10 ⁻⁴	0.85	720
Ti-6Al-4V-2Co	903	1499	2 x 10 ⁻⁴	0.53	670
Ti-6Al-4V-2Fe	815	1499	2×10^{-4}	0.54	650
Ti-5Al-2.5Sn	1000	1830	2 x 10 ⁻⁴	0.49	420
Nickel:					
IN 199 (PM)	1010	1850		0.5	1000
Iron:					
Fe-1.6C (+1.5Cr)	650	1202	10-4	0.46	1200
Fe-26Cr-6.5Ni (IN 744)	900	1652	5 x 10 ⁻⁴	-	1000
Zinc: Zn-22Al	200	392	10-2	0.5	2000

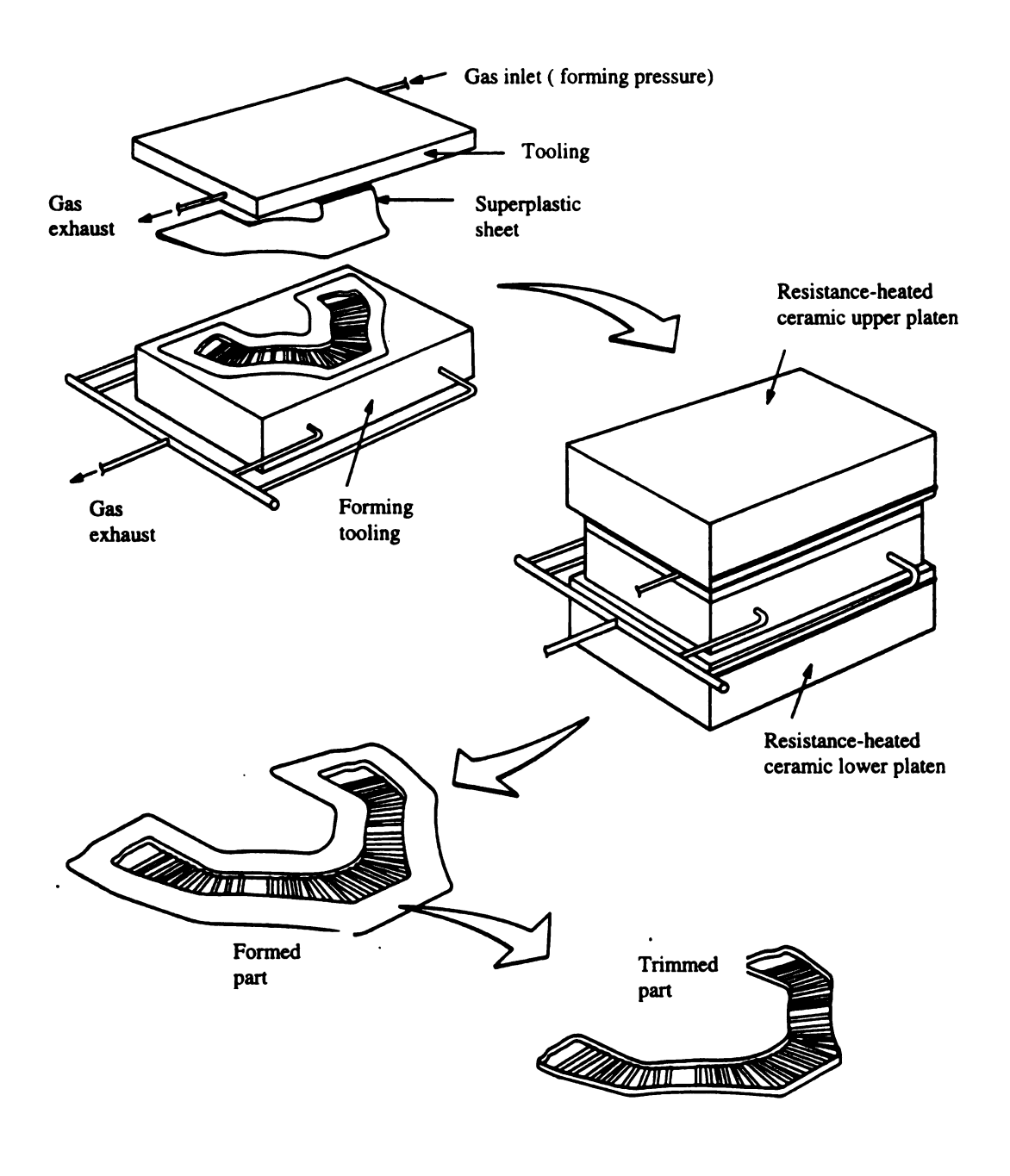


Figure 3. The schematic view of sequence for superplastic forming process [5]

The forming temperature is also important in superplastic forming, since the temperature variation in a forming die is a primary source of localized thinning.

Recently, a number of methods has been reported for superplastic materials forming [2,

- 5]. Each method has a unique capability and develops a unique set of forming
- characteristics. They are: (1) blow forming, (2) vacuum forming, (3) deep drawing,
- (4) superplastic forming /diffusion bonding, (5) forging, (6) extrusion and (7) dieless drawing.

Blow and vacuum forming are basically the same process in which a gas pressure is imposed on the superplastic diaphragm, causing the material to form into the die configuration. In vacuum forming, the applied pressure is limited to atmospheric pressure, and the forming rate and capability are therefore limited. With blow forming, additional pressure is applied from a gas pressure reservoir, and the only limitations are related to the pressure of the gas rating of the system, and the pressure of the gas source. Generally, large and complex parts can be formed by this method, because it has the advantage of no moving die components and dose not require mated die components. Multiple parts can be formed in a single process cycle, thus permitting an increase in the production rate for some parts.

Thermal-forming methods, adopted from plastic technology, sometimes use a moving or adjustable die member in conjunction with a gas pressure or vacuum. These techniques

provide many ways of producing different shapes of parts, and are effective for controlling the thinning characteristics of the finished part.

For deep-drawing process, it depends on strain hardening to achieve the required formability and to prevent thinning and rupture during forming. We know that superplastic materials do not strain harden to any great extent, but they depend on the high strain rate hardening for their forming characteristics.

Recent developments in superplastic forming have been demonstrated that a number of unique processes are available if joining methods, such as diffusion bonding can be combined with superplastic forming. This technique involves the use of a minimum of four sheets to make a sandwich panel. The external sheets are then bonded, the inner two sheets are then welded to define the core structure, and finally the core is expended to bond with the external sheets and to complete the formation of sandwich structure.

Forging is a closed die process for the manufacture of precise shapes. It is usually a high temperature process and occurs under conditions in which low flow stress is encountered. Superplastic alloys have very low stresses at low strain rate and although compressive tests have shown that frictional constraints can lead to pressure build up, the effect is much less marked than in compressive deformation of conventional alloys. Thus it can be anticipated that if sufficient time is allowed then the use of superplastic alloys in closed die forging should result in excellent die filling with efficient reproduction of very fine detail.

Chapter 3

PRINCIPLE OF LASER & LASER MATERIALS PROCESSING

3.1 Principle of Laser Operation

Lasers have evolved into an important element of advanced technology since T. H. Maiman created the first working laser in 1960 [33]. Laser is an acronym for light amplification by stimulated emission of radiation. Due to the highly directional, monochromatic and coherent nature of light emitted from a laser, many uses have been found for laser devices in ways never before imagined. Examples include powerful, effective tools developed for material processing such as in welding and cutting of steel, inspection of parts and checking dimensional tolerances, and many others. Other uses for lasers have been found in the field of medicine as a precise surgical tool, in chemistry for analytical techniques, and in electronics for communications and information processing [33, 44].

3.1.1 Radiation of Light Quantum

Light is a form of electromagnetic radiation exhibiting both wave and particle-like characters. Experiments originating in the later 19th century led to the development of a branch of physics called quantum mechanics which describes light energy in terms of quantized units called photons. The energy of a photon is related to its frequency by the relation

$$E = hv = hc/\lambda$$

Where ν is the frequency, c is the velocity of light, λ is the wavelength, and h is Planck's constant and has the value: $h = 6.627 \times 10^{-34}$ Joule-sec = 6.626×10^{-27} erg-sec.

3.1.2 Stimulated Emission

Emission of light from an atom occurs when an electron makes a transition from one energy state to another lower energy state. For one electron shifting from one orbit at energy level E_2 to E_1 , the energy of the emitted photon would be: $h\nu = E_2 - E_1$.

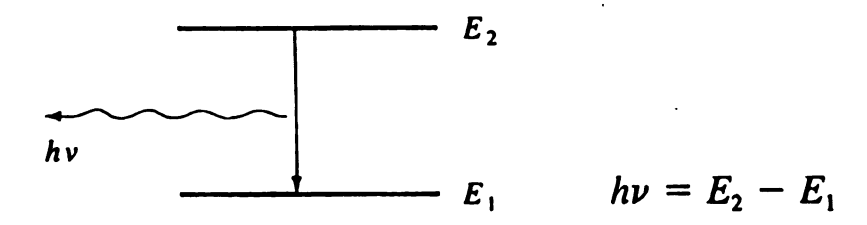


Figure 4. Spontaneous photon emission due to electron shift from a higher to lower energy level [41].

In a material at a finite temperature, there will be some electrons that are thermally excited to a higher energy levels through a random process. These electrons will fall back to lower energy levels, emitting photons. This process is classified as *spontaneous* emission because of its random nature. The rate at which electrons fall from some upper energy level E_2 is proportional to the population of electrons at this energy level. Given an initial number of electrons N_0 at an upper energy level, and with no replenishing of the supply, the population of electrons n_2 would exponentially decay. That is,

$$n_2(t) = N_0 \exp(-\alpha t) \tag{1}$$

Where N_o is an initial populatio of electrons at E_2 , and α is some decay constant.

Electrons can also be *stimulated* to fall from a higher to lower energy level. A photon field of the proper frequency provides this stimulus such that the energy of the photons corresponds to the difference in energy levels in which the electron is transitioning between.

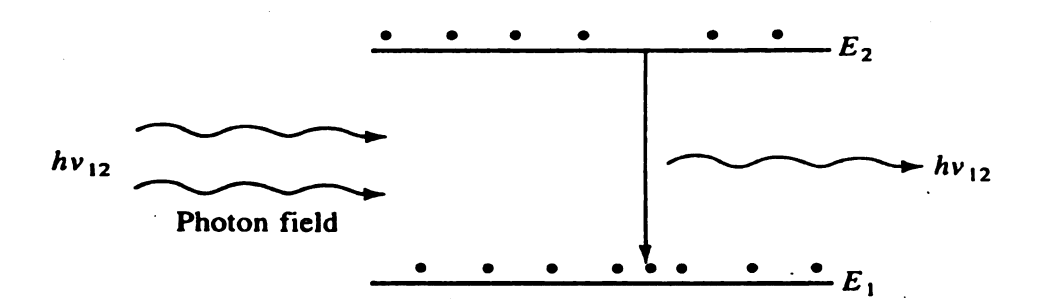


Figure 5. Photon stimulated transition of an electron and photon emission [41].

The rate of stimulated emission will be proportional to the population of electrons at energy level E_2 and the energy density of the incoming photon field, which we will denote as ρ_{12} .

Along with stimulated emission, absorption can also occur in which electrons are promoted from energy level E_1 to a higher energy level E_2 . This process would also be

proportional to the energy density of the photon field ρ_{12} and the population of electrons n_1 at energy level E_1 .

Now consider a steady state condition in which absorption is balanced by emission of electrons. Let the rate of absorption be denoted as $B_{12}n_1\rho_{12}$, the rate of stimulated emission as $B_{21}n_2 \rho_{12}$, and the rate of spontaneous emission as $A_{21}n_2$. The coefficients B_{12} , B_{21} and A_{21} are called *Einstein coefficients*. Einstein described the steady state relation:

$$B_{12}n_1\rho_{12} = A_2n_2 + B_{21}n_2\rho_{12}$$
 (2)
Absorption = spontaneous + stimulated emission

The corresponding diagram illustrate as Figure 6:

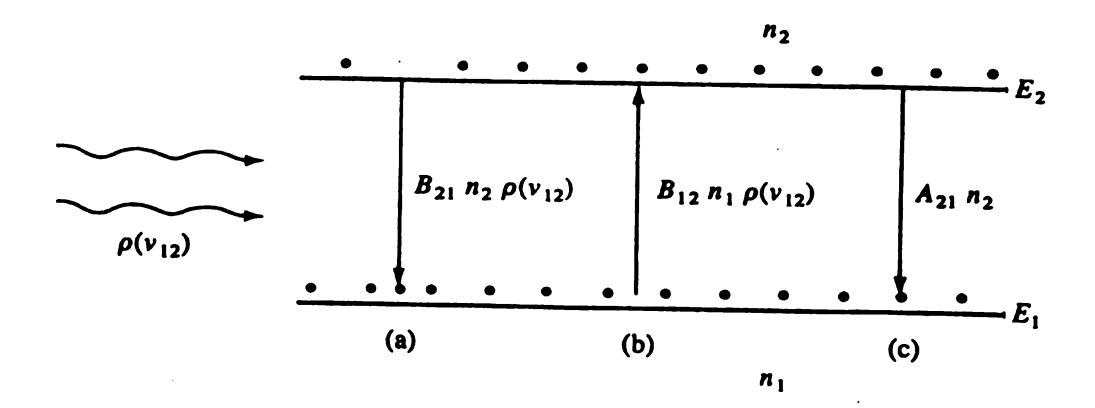


Figure 6. Balance of absorption and emission in steady state:

(a) stimulated emission; (b) absorption; (c) spontaneous emission. [41]

Because the stimulated emission corresponds to a definite energy transition, the emitted light is of uniform frequency, i.e., monochromatic. And because the stimulated emission would all be in phase, the emitted light is coherent.

From equation (2) we can deduce the condition necessary for increased stimulated emission. Obviously increasing the photon energy density ρ_{12} will increase stimulated emission, although absorption will likewise increase. Photon density increases can be achieved by the use of optical resonators. The other choice is to increase the electron population n_2 . However, we recall from statistical and thermal physics that the Bolltzman factor gives the ratio of electron populations at two different energy levels as

$$\frac{n_2}{n_1} = \exp\left[-\left(\frac{E_2 - E_1}{kT}\right)\right] = \exp\left(\frac{-hv_{12}}{kT}\right)$$

Assuming the density of available states is the same at both levels. k is Bolltzman's constant and it is equal to 1.38 x 10^{-23} Joules/K. Thus n_1 would normally be larger than n_2 as expected. Therefore, to increase stimulated emission significantly over absorption we would want n_2 to exceed n_1 . This condition is known as population inversion, or as a negative temperature condition.

3.2 CO₂ Laser

The laser, by definition, is a device that amplifies light by means of stimulated emission of radiation. In practice, a laser is generally used as a source or generator of radiation and the generator is constructed by adding a feedback mechanism in the form of mirrors to the light amplifier.

Amongst many types of lasers, the most important molecular laser is carbon dioxide laser [35]. Which means the CO₂ gas is employed as its active medium. The principle of lasing phenomenon of CO₂ laser can be considered as vibration energy, which provides various energy levels for laser transitions. It is known that the carbon dioxide molecule is a linear molecule and three atoms lie in a straight line with the carbon atom locates in the middle; Therefore, there are three different types of vibrations, which can occur in the carbon dioxide molecules. It is called as symmetric vibration, bending vibration and asymmetric vibration, which are illustrated schematically in Figure 7.

For the different vibration modes shown above, the energy associated with them is quantized. The molecule can vibrate in more than one mode at the same time and it can have more than one quantum of vibration energy in each mode. This feature leads to a simplified energy level schematic diagram shown in Figure 8, which is the most important mechanism for CO₂ laser operation. The population inversion in the CO₂ laser is produced through collisions with nitrogen molecules and high power output of CO₂ laser is obtained by adding nitrogen to the mixture. The nitrogen molecule is excited by collisions with electrons, and then transfers their energy from the collisions to CO₂

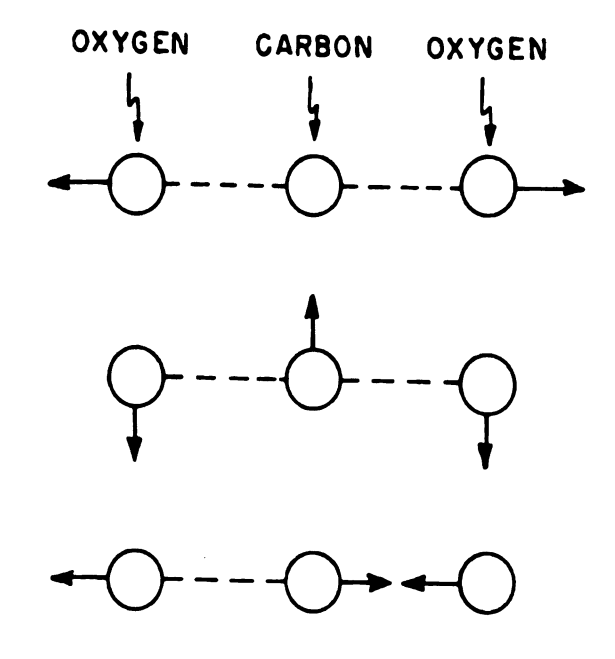


Figure 7. A vibration mode of CO₂ atoms [33]

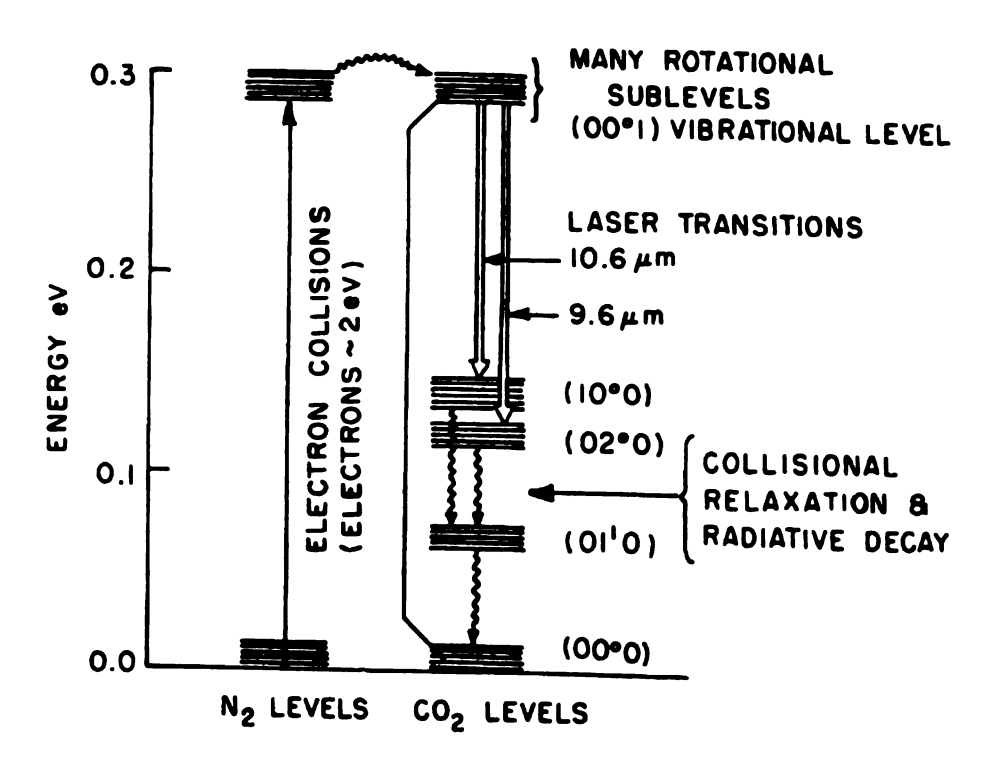


Figure 8. Energy levels of the CO₂ laser [33]

molecules. This produces a population inversion between the (001) state and the (100) state. Although there is another state (020), which shares a common upper state with the (001) state, the probability of transition to the (020) state is only about one-twentieth of that to the (100) state. The most of laser operation in CO₂ laser proceeds at the wavelength of 10.6 μm. The addition of helium to the gas mixture can also increase the output power. Because helium is a kind of gas, which tends to deplete the population on the lower laser level by collisions and tends to keep the gas mixture cool due to the high mobility of helium atoms. The cooling function of helium plays an important role in keeping the CO₂ lasers maintain a high power output situation. Therefore, in general, a CO₂ laser actually operates by utilizing a mixture of CO₂, N₂, and He together to obtain a high power output. This is the reason why CO₂ lasers are widely used in industries, and the CO₂ laser has been developed to produce a high power output up to 25kW recently.

3.3 The Characteristic of a Laser Beam

3.3.1 The Property of Continuous Beam

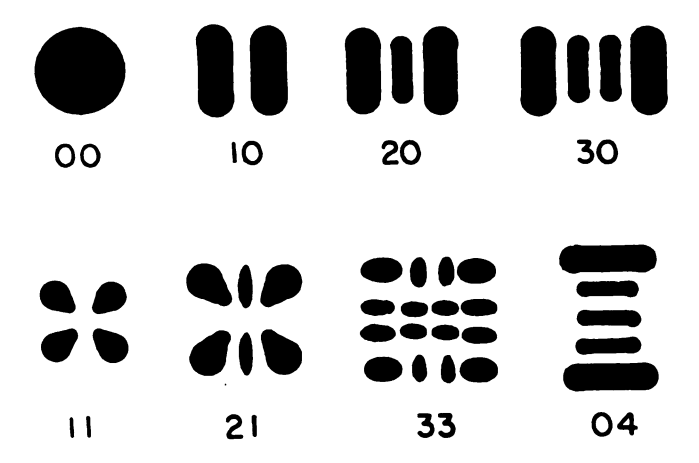
A laser with a continuous beam means that the output beam is constant, or the power output is measured as a constant wattage, so it is often called as "CW" laser. Many kind of gas laser can provide "CW" outputs. Since the gas can be operated to flow through the lasing chamber not only to replenish the gas but also to provide cooling function since the increase of the temperature of the gas mixture will decrease the power output. For example, in CO₂ laser, adding helium to the gas mixture in order to keep the gas mixture

as cool as possible, CW laser needs a relatively long period to establish beam intensity at constant output. Usually, the intensity is described as "power density", which has been defined in ANSI standard (the American National Standards Institute) Z 136.1 as below: "Quotient of the radiant flux incident on an element of the surface containing the point at which irradiant is measured, divided by the area of that element. Unit: watts per square centimeter, W/cm-2" [32].

3.3.2 The "Mode" of Laser Beam

The mode of laser beam is another important characteristic, which reflects the beam cross-sections, or spatial patterns. The distinctive spatial patterns are termed as "transverse modes". It describes the functional dependence of the electromagnetic field on X and Y coordinates. They are knotted as TEMmn modes, where the subscripts m and n represent the numbers and times the electric (or magnetic) field crosses the X and Y axes. In fact, the TEM mode indicates the amplitude distribution of the electric field in a plane perpendicular to the axis of the laser resonator. Some transverse mode patterns are presented in Figure 9.

From the Figure 9, it is obvious that the lowest order mode TEM_{00} , which is called as Ganssion distribution, has maximum power density no matter in rectangular or cylindrical symmetry patterns because of its small beam divergence angle. Therefore, it is the desirable mode for laser operation since the power density distribution is more uniform than higher order modes. Actually, the TEM_{01} mode, which is often called the



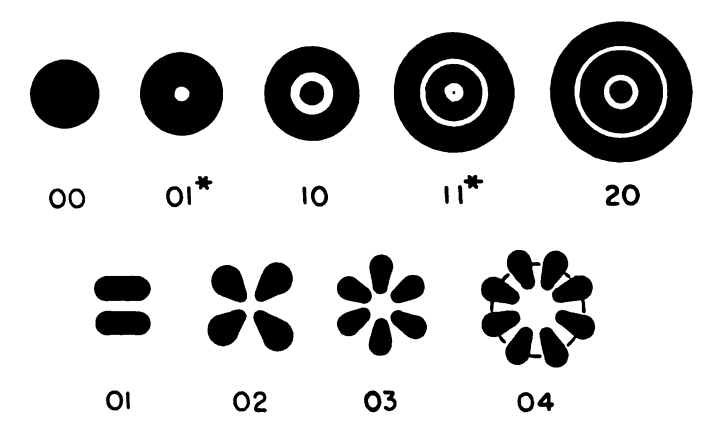


Figure 9. Transverse-mode patterns in rectangular symmetry (upper) and in cylindrical symmetry (lower). [34]

"donut mode" and is made up of a combination of TEM₀₁ and TEM₁₀, and it is commonly used in gas laser such as CO₂ laser operating at or above 1KW range.

3.4 Interaction of Laser Beam with Materials

In laser materials processing applications, the principle of interaction of the laser with material is to utilize lasers emitting photons with relatively low energy. For example, the energy of CO₂ laser photons is only 0.12 eV and the photons come from YGA laser have about 1.2 eV energy [35]. Thus, the electrons excited by CO₂ laser or YGA laser radiation does not have enough energy to be removed from the metal surface. They return to an equilibrium state when excited electrons are scattered by lattice defects, such as dislocation, grain boundaries, and other discontinues. The excess energy will be released to convert electronic energy obtained from the beam of incident photons to heat energy, which is used for laser materials processing. In fact, when the laser radiation shoot on the surface of a workpiece, a part of radiation is absorbed, and most parts of that are reflected. Just the absorbed part is capable of being effective in raising the energy state of the electrons within the metal so that the excited electrons collide with lattice atoms to create heat energy.

The result of heat transfer by laser radiation on the surface of metal lead to the surface temperature quickly rising to its melting temperature. This phenomenon is of interest for welding, cutting and other such applications. The temperature distribution of the metal surface interacted with laser radiation depends on the heat flow in the material. The heat flow depends on the thermal conductivity K and the specific heat of the material. The

heating rate is an important factor, and it can be expressed as the term of $K/c\rho$, where ρ is material density. This term has the characteristic of a diffusion coefficient since its dimension is cm²/sec. Hence the heat flow can be calculated by using the usual heat diffusion equation.

The Figure 10 illustrates a surface temperature of Aluminum as a function of time for various absorbed energy densities [39]. The reflectivity of a metal surface is another important parameter in laser materials processing. It is very sensitive to the status of the surface such as impurities, oxide layers and the nature of the metals as well as the wavelength of laser beam. The reflectivity of several metals as a function of wavelength is shown in Figure 11.

From Fig. 11, it is obvious that aluminum has a very high reflectivity through the visible spectrum, but ferrous metal such as steel and Nickel alloys have relatively lower reflectivity throughout the entire spectrum. Another phenomenon shown in Fig.11 is that the reflectivity of the surface is especially important for CO₂ laser due to its wavelength at 10.6 µm. It is difficult to couple the energy from the optical beam into the workpiece. Therefore, how to improve the absorption of infrared CO₂ laser energy is the first problem need to be solved. Up to now, there are couple of treatments used for enhancing the absorptivity of metals at 10.6 µm wavelength of CO₂ laser. In industrial application, surface coating, and surface oxidation have been used to increase absorption [36, 37]. It

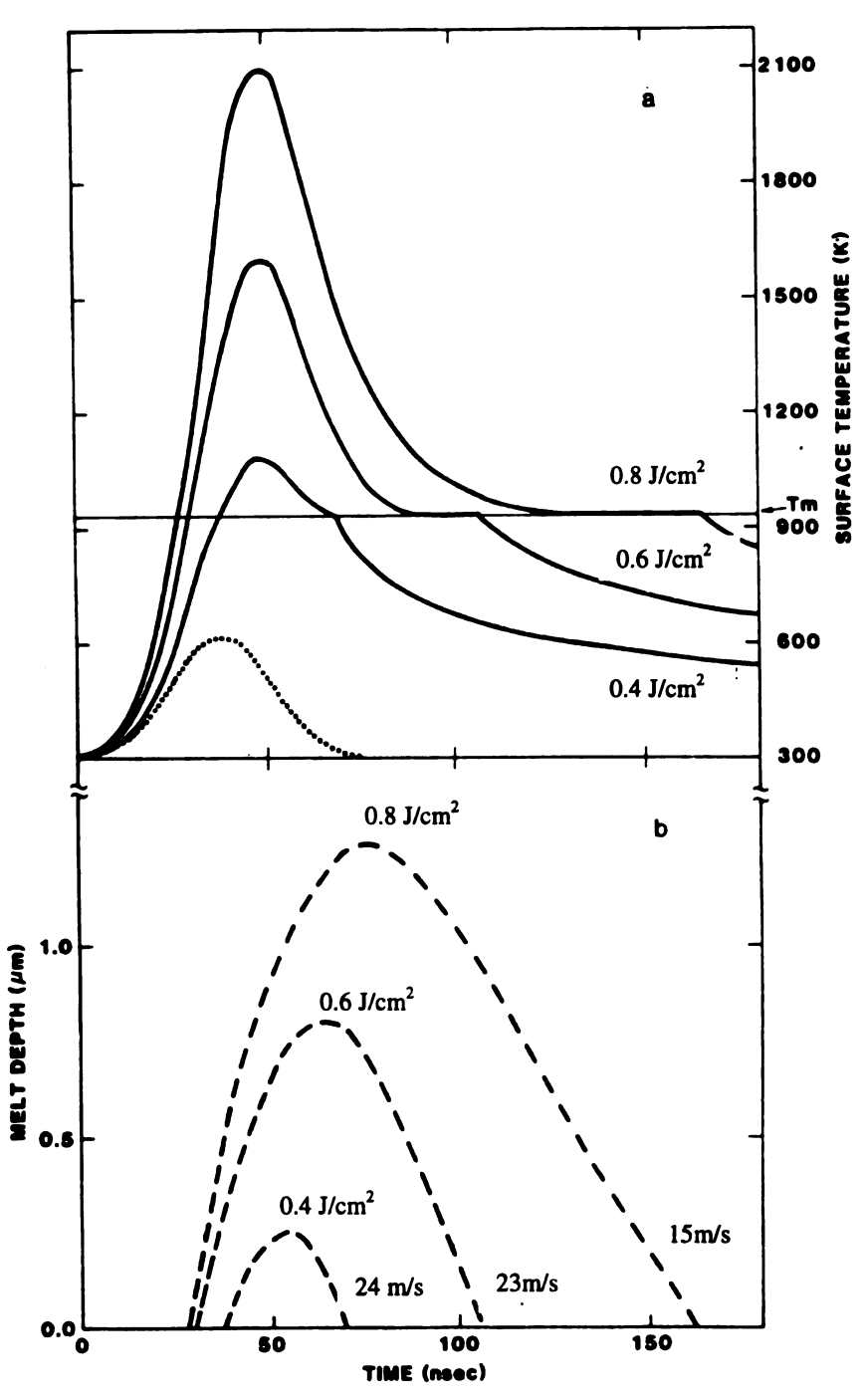


Figure 10. Surface temperature of Al as a function of time for various absorbed energy.

The dotted line shows the shape of the Gaussian laser beam mode. (upper)

Melt depth as a function of time with velocity of the liquid-solid interface.

(lower) [39]

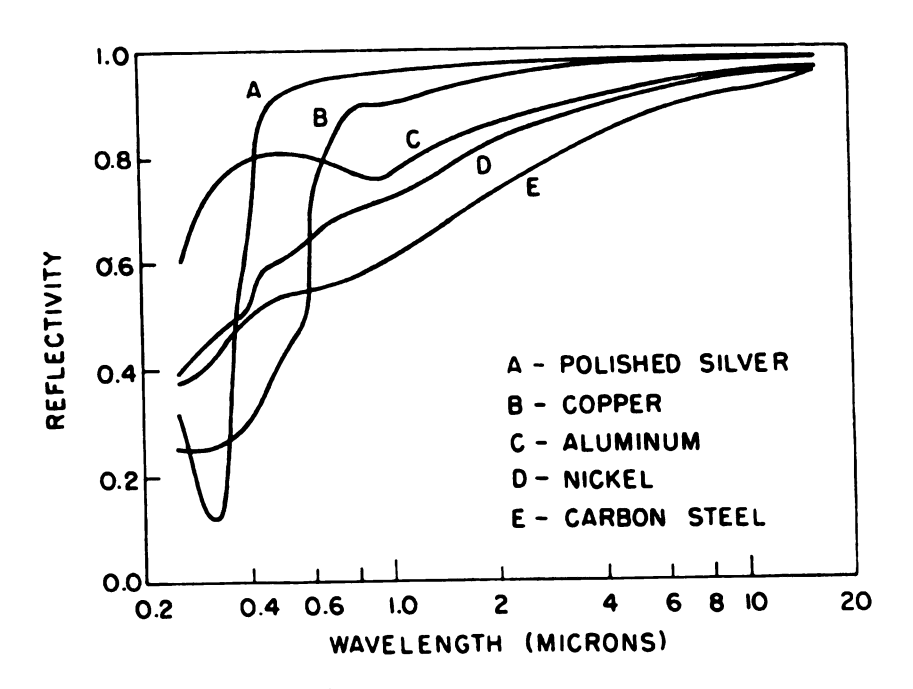


Figure 11. Reflectivity as a function of wavelength for several metals. [35]

has also been partially improved by roughing, etching, and baking at certain temperatures through our experiments [38].

3.5 Laser Applications in Materials Processing

Comparing to a conventional thermal source, a laser can deliver very high power density to a localized region on a workpiece. For example, a metal can not be melted by a 200 w light bulb but a 200 w continuos laser can do that. Therefore the laser has become a source of energy that can be concentrated by a series of lens (or mirrors), achieve very high power density at the focal spot. This ability provides many potential applications in materials processing technology.

3.5.1 Laser Cutting

Laser can be used to cut a wide variety materials. Laser cutting will cause a vaporization of materials along a path, which is created by a moving laser beam, and it leads to separation of the pieces. Because CO₂ laser with 10.6 µm wavelength beam can be manufactured with extremely high continuos wave power densities. It is most commonly used in industrial cutting. Not only in cutting of metals, but also in nonmetals materials such as ceramics, plastics, cloth, wood and paper, and glass [40,43,47]. Gas jetting is usually associated with metal cutting either to enhance the removal with a reactive gas, such as oxygen, or with an inert gas to protect flammables. Because of high reflectivity, some metals that are efficiently cut with the CO₂ lasers, such as aluminum and titanium[46, 47,52, 54].

3.5.2 Laser Welding

Laser welding technology has been considered ideally suitable for welding plastic materials, ceramics, glass and metallic materials. Because the localized nature of the laser beam, the heat affected region can be kept to a minimum size so that the welding zone is able to keep the surface clean and unaffected. The technique of laser welding is to utilize the rapid interaction of material with a focussed laser beam. A big difference between the melting temperature on the surface and an ambient temperature inside the substrate forms a steep temperature gradient, which is an important principle of creating rapid solidification. The power density, traverse speed, interaction time and pressure of cover gas are main parameters influencing the solidification and quench rates that influence the quality of welding. Compared with some established techniques, there is some advantage in laser welding. For example, no material contacts the workpiece, so that there is no contamination. The heat-affected zone is very small. It is especially important for the cases where a weld must be made near a heat sensitive element. Another example is that laser welding can be performed under the ordinary atmosphere, which is big cost saving. Because of these advantages, laser welding is gaining more and more acceptances for performing welding tasks [48-51, 58, 59].

3.5.3 Laser Surface Treatment

Laser surface treatment includes laser hardening, remelting, alloying and cladding processes. Recently, these techniques are widely applied in industry due to their interest features. A high power density is created on a small area on the top of the alloy so that a very rapid heating and cooling occurs near the surface of materials. For the laser

hardening ferrous alloys, a phase transformation can occur from austenite to martensite due to vary rapid cooling. After transformation, the hardness on the surface layer increases because a certain volume fraction undergoes the phase transformation, which lead to a surface hardening [39, 41, 47, 55, 57].

For laser remelting, its purpose is to improve the wear resistance and corrosion resistance of the surface of materials. This is because that the microstructure of the surface can be changed due to the rapid self-quenching process. Laser alloying is another way of changing the chemical composition and microstructure of the surface. Simultaneously, with surface melting, an alloying element can be injected to obtain a new alloying layer. Majority of alloying elements like C, Ni, Cr, Mo, W, Co, Mn, and Ti are usually used for improving properties of the surface in steels [60, 61, 62], aluminum alloys [63, 64], and titanium alloys [65, 66].

Laser cladding is also widely used in industry for obtaining a high hardness, high wear resistance, high corrosion resistance and high-temperature resistance without affecting the substrate material. The mechanism of laser cladding is that an alloy powder or metal/carbide mixtures, such as SiC, TiC, and VC [67], are injected along with a laser beam, resulting in a rapidly solidified cladding layer which coats the surface of the substrate. Generally, a perfect clad has characteristics of uniform coating thickness and smooth surface, minimum dilution and distortion, as well as good metallurgical bonding with the substrate.

3.5.4 Laser Forming (Bending)

Although laser forming is a relatively new technique comparing with other laser materials processing, but it is also a big development in this field of study. It could potentially be used for tool-less manufacturing parts necessaries for automobile and aerospace industry [68, 70, 71, 73]. The microscopic scale applications of laser forming are also involved in stereolithography [72], and micro-optical components field [74]. However, the principle mechanism of laser forming, in the microscopic scale, is that the sheet metal is heated by the laser beam, and the forming temperature is controlled by adjusting the power output parameters and path feed rate. The gravitational force, a positive or a negative pressure work as forming stresses, which influences the shape change operation.

In this research, we have demonstrated, for the very first time, that a laser-aided 3-D forming of a superplastic material is possible. The review part of this thesis describe this development.

Chapter 4

LASER DIELESS SUPERPLASTIC METAL FORMING

Laser Die-less Superplastic Forming (LSF) is a novel laser processing technique. To our best knowledge, such a forming process has not been reported to date in any of the recent reviews [75-77]. The new possibility of this technology can be realized by combining the innovative "tool" - laser beam and metal forming without any mechanical contact. Comparing with conventional superplastic forming, which is accomplished by using die pressing or extruding to force the metal sheet into a die cavity when the temperature of the sheet reaches deformation temperature, the hard tooling is not required. Therefore, it is high technology process and an economical processing technique especially for rapid prototyping and small batch productions.

4.1 The Function of Laser Beam

The utilization of high-energy laser beam for plastic and superplastic forming opens another application in laser materials processing field. The physical fundamentals of laser action, during forming process, is based on the localized heating of the surface of a metal sheet. A controlled laser beam is applied at selected, and preprogrammed locations on a superplastic sheet. The sheet metal is heated by the laser beam, and the deformation shape is obtained by a slow scanning laser beam along a programmed pattern. It is possible to achieve an ideal forming component by adjusting the parameters such as laser

power, laser beam size and transverse speed of the beam. Figure 12 is a schematic diagram of CNC laser assisted superplastic forming.

4.1.1 Laser Beam Power

Laser beam power is one of the primary factors, which influences the quality of laser processing. The combination of incident laser power and relative beam size constructs the power density within the radiation region.

In laser superplastic forming process, the interaction between laser beam and metal sheet provides the heat to metal sample. Therefore, the laser energy works as a heating source for reaching a deformation temperature. However, the amount of laser energy required to achieve a suitable deformation temperature is the most critical issue. Due to a high reflectivity of Aluminum alloy to the infrared CO₂ laser radiation, the key point for inducing laser energy to create a required temperature on the surface of workpiece is to manage to improve the surface condition. There are some methods for improving the absorption condition have been tried, such as roughing, etching, polishing, anodizing and painting [77, 78].

4.1.2 Laser beam diameter

Laser beam diameter is another important variable, which influences the power output.

This means that the power density will vary with this variable directly. Theoretically, the light emitted by laser is confined to a rather narrow cone, with a diameter "d", but as the

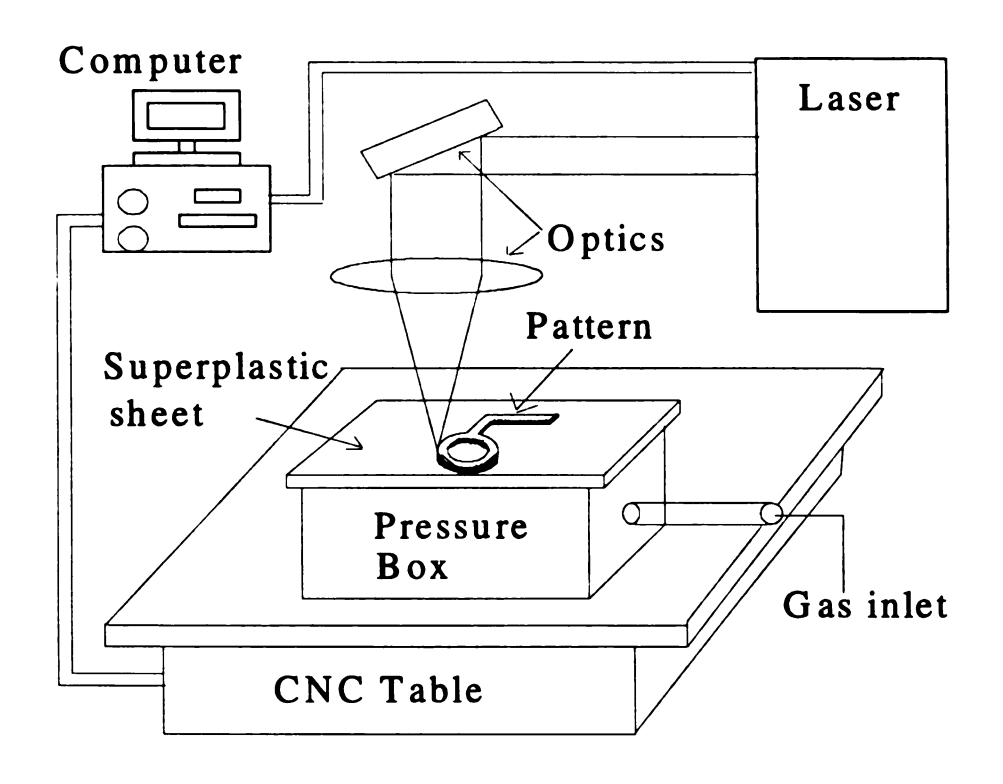


Figure 12. Schematic diagram of CNC laser assisted superplastic forming

beam moves through space, it slowly diverges to a bigger diameter "d". Simply, the relation between them is expressed as

$$D' = 1\theta + d$$

Where I is the traversing distance of laser beam, θ is a small divergence angle. The CW gas laser generally has the smallest values of beam divergence. So in fact, the laser beam diameter is usually adjusted by changing the distance between the beam jet (beam head) to the surface of the workpiece. In addition, since the characteristic of laser beam "mode", it is also an obvious factor, which affect the laser energy distribution in the interaction zone. As described as before, the TEM₀₀ "mode" or Gassion Distribution is an ideal mode because its uniform energy distribution in the spot area. For CO₂ laser generator, TEM _{01*} mode is commonly used for laser materials processing. For laser forming application, TEM _{01*} mode is also effective for creating a uniform energy distribution on the surface of the metal sheet because of its "donut" pattern.

4.1.3 The Beam Traverse Speed

A successful laser-aided superplastic deformation just can occur at a certain condition with a critical combination of optimum parameters including power output, beam diameter and traverse speed.

Due to the high thermal conductivity of Aluminum alloy, it is difficult to establish a relatively stable temperature distribution around forming zone. The heat is applied within small area at a time, a proper sequence of heating zones could be mapped out individually

and the sum of these locally deformed areas will result in the final shape of the element. For avoiding a non-uniform deformation, this is caused by combining much localized deformation. An effective way to avoid that is to decrease the beam traverse speed, and increase the beam spot size to provide sufficient energy, which can be transferred to heat at a certain time for keeping the temperature distribution as uniform as possible within the heating zones.

4.1.4 Beam Scanning Track

The feature of the laser dieless superplastic forming is that no mechanical contact exist. The geometry of the heating path and the amount of the heat input have been precisely implemented through designing a beam scanning track, which is programmed by using CAM/CAD package to run the computer controlled table under the laser beam. It is possible to realize a dieless superplastic forming by moving laser beam scanned on the target of forming part. According to its mechanism, the beam scanning track akin to the function of tooling die used in conventional superplastic forming technique.

4.2 Forming Force

The term of "die-less" has indicated that in laser superplastic forming technique, a mechanical contact is not required. The stress needed to deform the sheet metal is applied by a vacuum or an inner gas in a cavity container. Comparing with the conventional superplastic forming technique, using gas as forming "die" instead of mechanical forming die is an innovate idea, which provide a more uniform stress distributing throughout the action region of the workpiece. It is a highly desirable feature, since the corners of the

forming parts usually have the thinnest section in conventional superplastic forming especially for a complex part. There are some shortcomings of the gas forming. For example, the applied vacuum is limited to the pressure of atmosphere, or the inner gas added in the cavity chamber could not be put too much due to the resistance to pressure of the chamber. It has also a strong potential to provide a sufficient forming force to produce complex shapes component without the use of dies. Furthermore, this technique will offer a prospect to control the thickness uniformly at any part of the final shape.

Chapter 5

EXPERIMENTAL PROCEDURE

In this research, a high energy laser was employed as a heating resource to aid in shaping superplastic sheet metal. The heated superplastic sheet was deformed by either applying a vacuum or by an argon gas pressure. The desirable deformation shapes could be obtained by programming the computer numerically controlled (CNC) code, which drives the CNC table to move the sample with respect to the laser beam. So, the feature of the laser-dieless forming processing, is that a deformation temperature, could be controlled by adjusting the power of laser energy, and the geometry of the heating path could be precisely controlled through computer assisted manufacturing (CAM) system.

5.1 Experimental Setup

The equipment used in the experiments, consist of a continuos wave CO₂ laser generator, a computer - assisted manufacturing (CAM) system, and a forming chamber. The experimental setup is shown in Figure 13 and Figure 14.

5.1.1 **CO₂ Laser**

A 2500-L model Triumph (Triumph Industrial Laser Inc., MA) laser in the TEM _{01* mode} is being used in this study. The characteristics are given in Table 2. For superplastic forming experiments, the amount of the heat transferred from laser energy to the work

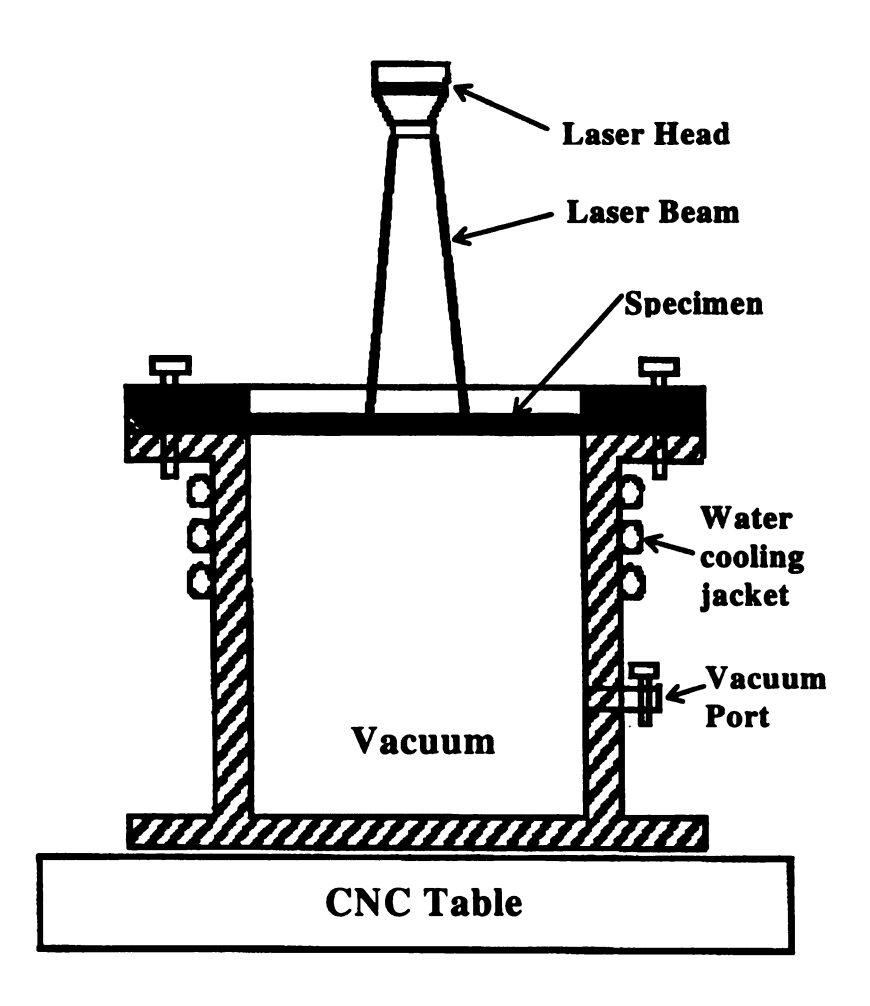


Figure 13. Schematic diagram showing the vacuum chamber used in conjunction with laser processing



Figure 14. A photograph showing the laser nozzle, the chamber, and the temperature measuring setup.

piece is an important parameter. According to the temperature measurement, the output power range of 200 to 500 watts was used during this processing.

Table 2. The Characteristics of the (TRUMPF 2500 W) RF exited CO₂ laser

Parameter	Value/Type
Type of Laser	Fast flow coaxial CO ₂ laser
Mode of the beam	TEM ₀₁ •
Output stability	± 2 %
Beam diameter (raw)	≈ 18 mm
Excitation	RF exited
Temporal mode	Continuous and pulsed (1-10kHz)
Maximum output power	2800 watts (continuous)
Wave length	10.6 µm
Gas consumption	He: 64 l/hr
	N2: 12 l/hr
	CO ₂ : 31/hr

5.1.2 CAM System

A computer - assisted manufacturing (CAM) system was used for laser dieless superplastic forming experiments. This system consists of a high precision X-Y table controlled by a computer numerically controller that is called CNC table machine.

(General Numeric Inc.) Its specifications are given in Table 3. Generally, for laser materials processing, the specimen is fixed on the X-Y table which can move under a stationary laser beam. The designed pattern on the metal sheet is realized by moving X-Y table. A CAD package is used to design the scanning path.

Table 3. Specifications of the CNC machine

Description	Value		
Range of motion	1.27 m x 1.27 m		
Maximum contour speed	0.127 m/sec	 	
Maximum traverse speed	0.254 m/sec		
Accuracy	0.0166 cm/m		
Resolution	0.0127 cm		
Repeatability	0.00254 cm		

5.1.3 Superplastic Forming Process

A novel superplastic forming system was designed by our lab. It consists of a vacuum pump, a vacuum chamber (\$\phi\$ 4.0 inch x 5.0 inch) with cooling water tubes, which are wrapped around the wall of the chamber. A vacuum gage or a pressure gage could be connected to the chamber. The chamber was made of steel, and the capability of loading pressure is over 2.0 bar, which is the highest pressure that was used in the experiments. The forming system setup is shown in Figure 15a, and 15b, where Figure 15a shows the

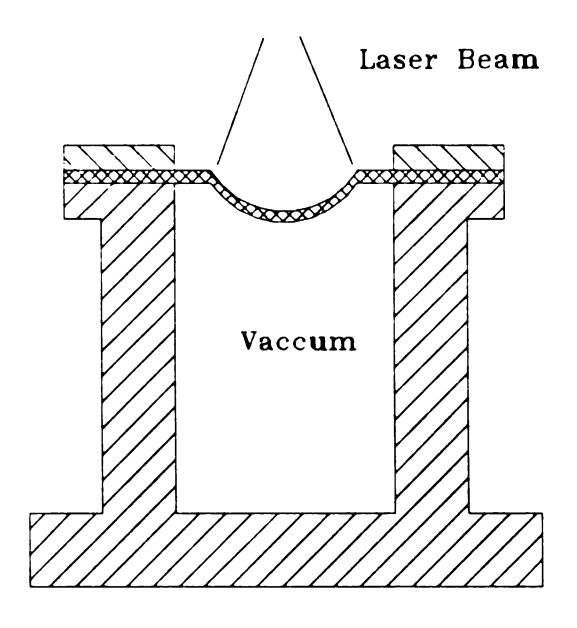


Figure 15a. A schematic diagram showing the condition of vacuum forming

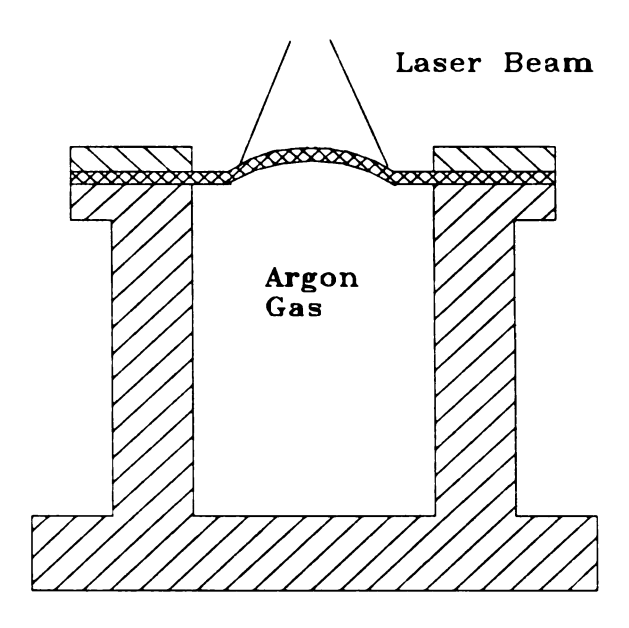


Figure 15b. A schematic diagram showing the condition of argon gas forming

conditions that vacuum was applied, and the Figure 15b sketched the conditions for an argon gas pressure induced superplastic forming.

5.1.4 Measurement System

For the temperature measurement, we used a computer data acquisition system, which is connected with four pair of thermocouples. The thermocouples were connected to points on different locations from the center of the metal sheet. This is to measure the temperature distribution and to view the inference of thermal conductivity of the sample. A sketch of the temperature measurement system is shown in Figure 16.

A profiler was used to trace the deformation progress of metal sheet during different stages of the process.

An OLYMPUS PME-3 optical microscope was used to evaluate the microstructure and grain size of the samples. For the measurement of the thickness variance, a precision optical measuring tool was used for the cross-section analysis.

5.2 Preparation of the Testing Materials

We used different kinds of testing materials in the experiments. However, since the requirement for superplastic deformation, relatively a few materials are able to qualify. Thus, our range of choice is relatively narrow. In this research, the 7475 aluminum alloys, 5083 aluminum alloys, and GK 45 aluminum alloys were tested.

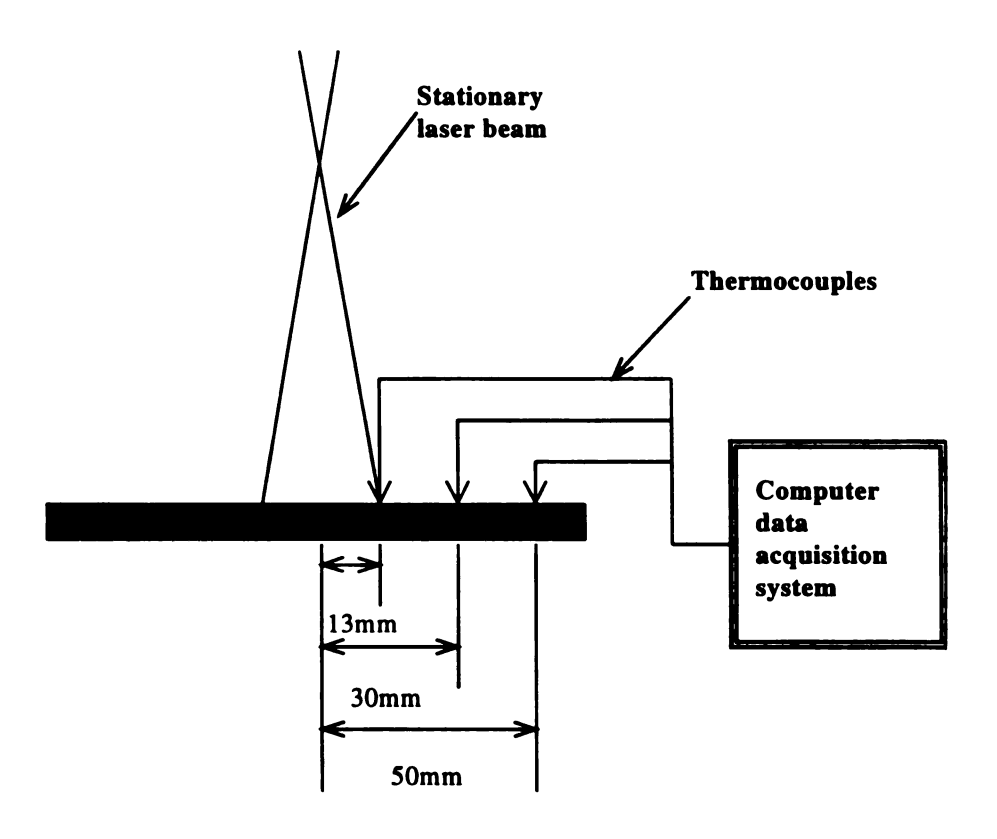


Figure 16. A schematic diagram showing the setup for temperature measurement

In addition, the 718-Nickel based alloy, and a thermal-plastic polymeric sheets were also tested. After preliminary tests of various materials, we focused on GK 45 aluminum superplastic alloy, that has the right properties for this process.

It is well known that aluminum has a very low absorption of infrared CO₂ laser energy. Since the aluminum sheets, received from Japan, were cool-rolled, they exhibited shinning surfaces. At first, the absorption of infrared CO₂ laser energy on their surfaces was a problem.

In order to improve the surface condition of the aluminum sheet for higher absorption of laser energy, different methods were used. First, a high temperature black paint was applied on the surface. However, the paint easily peel off from the surface during the laser heating and processing. This shows that the bonding between the black paint and the surface was very poor. Second, before applying black paint, the surface of the sample was roughened with a coarse emery paper, and then sprayed with the high temperature black paint, This procedure was also not effective for getting stable condition. Finally, a very strong and cohesive bonding was achieved by using the following steps:

- Etching the surface of the sample prior to application of black paint where etching reagent was Barker's reagent.
- 2. Painting an uniform coat of high temperature black paint.
- 3. Curing the sample at 200°C, for 2 hours and cooling it in the air.

The chemical composition, and selected mechanical properties of GK 45 aluminum alloy are listed in Table 4.

Table 4. Composition and selected mechanical properties of GK 45 alloy

Compositions					Yield	Tensile	Strain Rate	Deformation
(wt %)					Strength	Strength		Temperature
Al	Mg	Mn	Cr	Zr				
Bal	4.5	0.6	0.2	*	125 MPa	285 MPa	$10^{-4} \sim 10^{-3} \text{s}^{-1}$	500~550°C

^{*} Not provided by the manufacturer

5. 3 General Description of Experiments

The first step of the experiment was to check the laser system, including processing in the Helium, Carbon Dioxide and Nitrogen gases. Further, turning on the cooling machine, and checking the optics. After checking, if this conditions were normal, then turning on the laser beam and adjusting output power. Next step is to install the sample on the top of vacuum chamber, and the chamber is then fixed onto the CNC table. The CNC table could be moved by controlling the CNC code transferred from the program. These different geometric shapes of deformation were obtained by moving the CNC table, with respect to the stationary laser beam.

Designing a deformation trace is an important procedure in which a desirable geometric pattern was generated by using a CAD (computer assisted design) package. A CAM (computer assisted manufacturing) program was then used to translate the CAD drawing to G-code program used by the CNC controller. The CNC table was driven by the CNC controller so that the sample on the top of the chamber which fixed on the CNC table

could be moved with respect to the stationery laser beam. The Figure 17 illustrates a simple pattern to get a dome-shaped deformation. The heating trace, for such a case, a circular pattern, and the *** of the dome is defined along the edge of the laser beam trace. A steady-state superplastic forming temperature, for the alloy, can now be established by adjusting the laser beam scanning speed, and laser power.

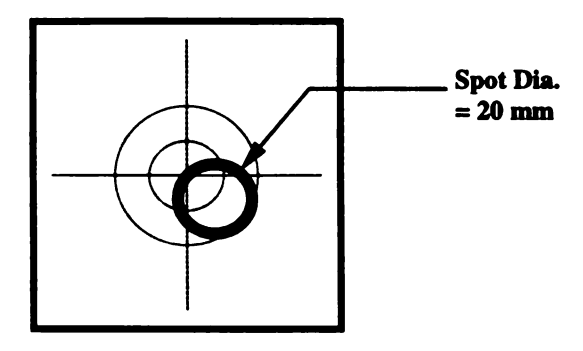


Figure 17. A schematic diagram showing the laser spot size, and the locus of the spot for generating a dome.

At the end of every program execution, a surface profiler was used to measure the progress of the deformation, and to see how much total deformation had been achieved.

Chapter 6

RESULTS AND DISCUSSION

6.1 Investigation of Laser Energy Effect

In any Laser-Aided materials processing technique, such as laser cutting, laser welding, and laser cladding as well as laser treatment, the amount of the laser energy absorbed by the material is a critical parameter. Especially for laser dieless superplastic forming, the amount of energy absorption from laser plays an important role in heating and cooling of the sheet metal. Thus, how much laser energy, which would be effective on the surface of the aluminum sheet, was initial consideration in this case. The high thermal conductivity of aluminum alloy is a critical component of this process.

6.1.1 The Influence of the Laser Parameters to Deformation

The power output, and the laser energy absorption are primary factors which influence the deformation. Laser dieless forming means that the laser will be the only heat source, which can raise the temperature to a proper region. In general, energy density is an important parameter used to evaluate the effectiveness of energy parameters in laser materials processing. Therefore, the concept of the "energy density" was introduced to design our experiments.

From the definition of the energy density

$$E_d = P_d \tau, \tag{6-1}$$

Where E_{d} energy density (J/cm²), P_{d} is the power density, and τ is the interaction time (sec), which is defined as the time required to move a distance of the laser beam diameter along the transverse direction.

Likewise, power density is defined as

$$P_d = P/A, (6-2)$$

where the P is the laser power (watts) and A is the irradiation area (cm²). Combining equation [6-1] and [6-2], energy density of circular density laser beam can also be expressed as follow. for a circular beam:

$$E_d = 4 P/\pi D v \tag{6-3}$$

where **D** is laser spot diameter (cm), and **v** is beam traverse speed (cm/sec).

It is obvious that the energy density is related to the beam diameter D, beam traverse speed v, and power output P. Finding a better combination of these parameters, for creating a possible deformation, will be our next concern.

6.1.1.1 Small Beam Diameter at Different Traverse Speed.

Theoretically, a fast scanning speed can decrease energy density, and a small diameter will increase the energy density according to the definition of the laser energy discussed before.

_

To look at the influence of power output **P** and traverse speed **v**, a 7475 aluminum alloy sample was first examined under a 5 mm diameter laser beam. The beam traversed speed is listed in Table 5.

The effects of laser energy absorption on the surface of six samples, arranged from #1 to #6, are shown in Figure 18. From this photograph, the first phenomenon is that the samples from #1 to #5 were partially melted in varying degrees, and the #5 sample is

most deeply melted. The second thing is that the #6 sample looks like very little or no melting at all. Since the energy density is related to P, the higher power is associated with the higher energy density. So for the highest power output P, which is 430 W, produces melting such as the appearance of the #5 sample. However, the #6 sample was treated at the same power output as the sample #2, at 320 W, but the traverse speed was almost four times slower than that in the #2 sample.

Table 5. The parameters used in the experiment for testing energy absorption

Sample number	Power output	Traverse speed
#	(watt)	(mm/s)
1	270	85
2	320	85
3	370	85
4	420	85
5	430	85
6	320	12

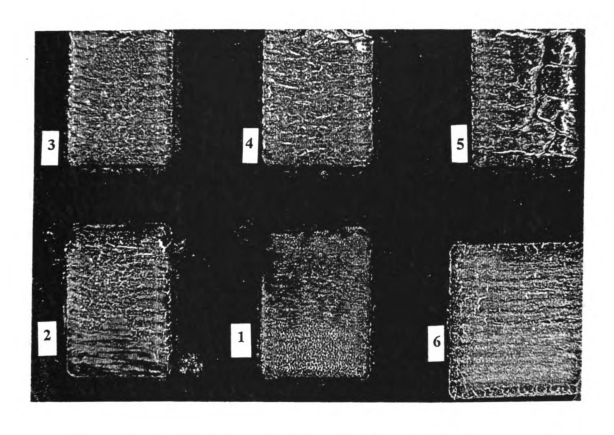


Figure 18. A Photograph of six patterns showing the surface condition associated with laser energy absorption. A small laser beam diameter with different traverse speeds used. Testing material was 7475 aluminum alloy.

Figure 19 is another photograph, showing a sample of 7475 aluminum alloy. The scanning pattern is a circle of diameter 38.1 mm (1.5 inch). The 405 W laser output, 5 mm spot diameter, and 0.423mm/s scanning speed were used in this sample. The running time is about 18 minuets. From the appearance of the heated surface (Figure 19), there was no melting, and a crack formed. This observation indicates that although the temperature was not high enough to melt the sample surface, a complicated internal stress field developed.

6.1.1.2 Large Beam Diameter

Based on the fact that the small laser beam size could not work properly, a larger beam spot diameter of 20 mm was tried. One pair of thermocouple was connected to the bottom of testing sheet, which was located at the point off the sheet center about 3 mm. The temperature variation with time are shown in Figures 20, 21 and 22.

From the curves shown in the Figures 20, 21 and 22, it is clear that the period of two peaks (shown in Figure 20) is about 120 seconds, and in Figure 21 this is approximately 140 seconds. For a power output of about 480 W and beam traverse speed of 0.105 mm/s, the period of the peak is over 600 seconds. In addition, the beam traverse speed alone could not achieve the highest temperature at certain power outputs. Therefore, this is another evidence that the laser energy coupling with aluminum is a complicated task. If the traverse speed remains at the same value, like the conditions shown in Figures 20

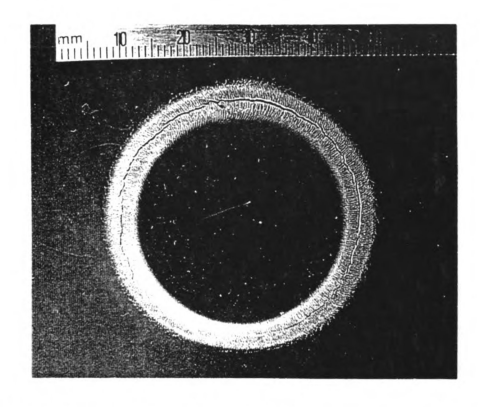


Figure 19. A photograph of a sample showing the surface condition associated with laser energy absorption on a circular pattern in a 7475 aluminum alloy.

Improper thermal conditions produce a circular crack.

and 21, the power output would be a primary factor to influence the steady state temperature distribution.

From the results of the two situations (small spot size and large spot size), it is seen that for a larger spot diameter is effective as a heating source to provide an uniform temperature distribution.

6.2 Measurement of Temperature Distribution

From the discussions in the previous section, it is clear that the temperature distribution in the area of the laser interaction is the most important condition in the dieless superplastic forming. In a conventional process, the heat provided by tooling die can create a uniform temperature distribution on the workpiece. However, there are two reasons why it is a somewhat difficult and a complex processing technique for laser dieless forming. One is that the heat resource comes from infrared CO₂ laser energy, which is highly reflected by aluminum alloy. Another reason is the high thermal conductivity of aluminum alloy, which makes it very difficult to establish a steady state temperature distribution.

6.2.1 Two Points Measurement (dynamic state)

Two points temperature distribution measurement is a basic idea to look at the heating conditions. Laser energy output is set to 230 W with a 5 mm diameter spot size.

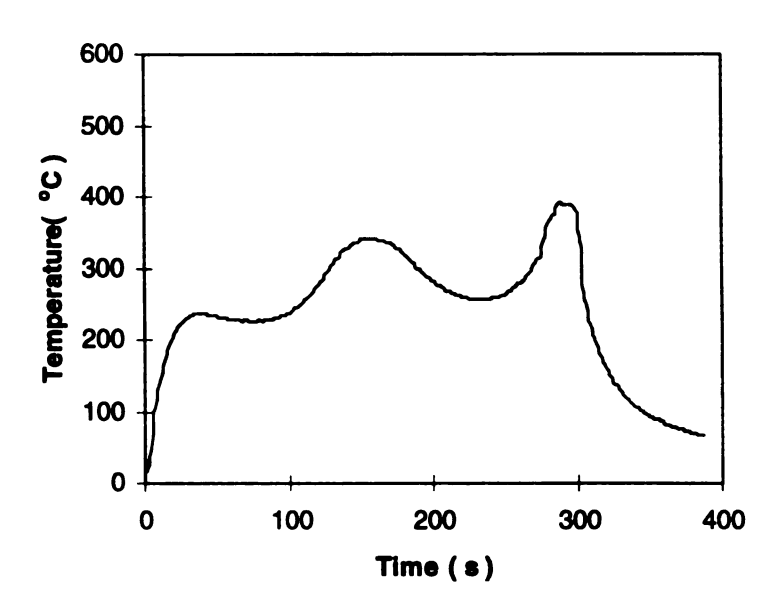


Figure 20. The temperature variation with 20 mm laser spot diameter, at 350 W power output, and a traverse speed at 0.42 mm/s.

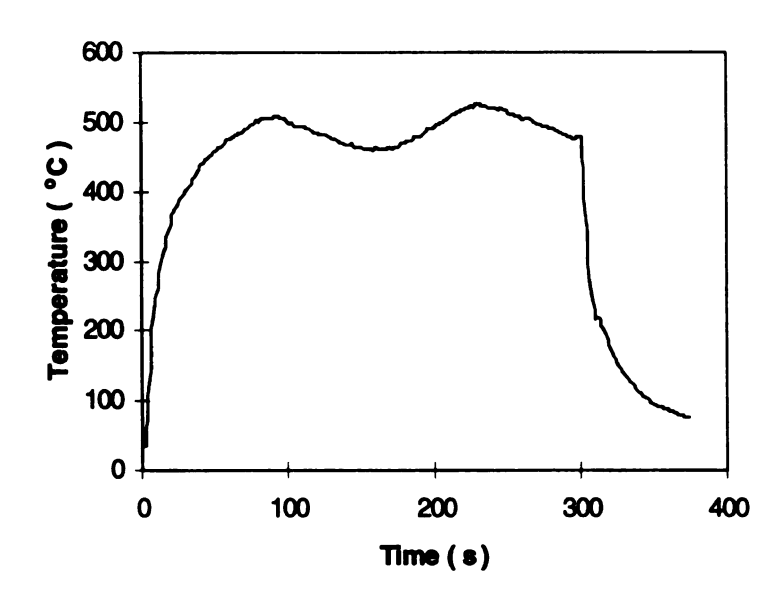


Figure 21. The temperature variation with 20 mm beam spot diameter, at 470 W power output, and a traverse speed at 0.42 mm/s.

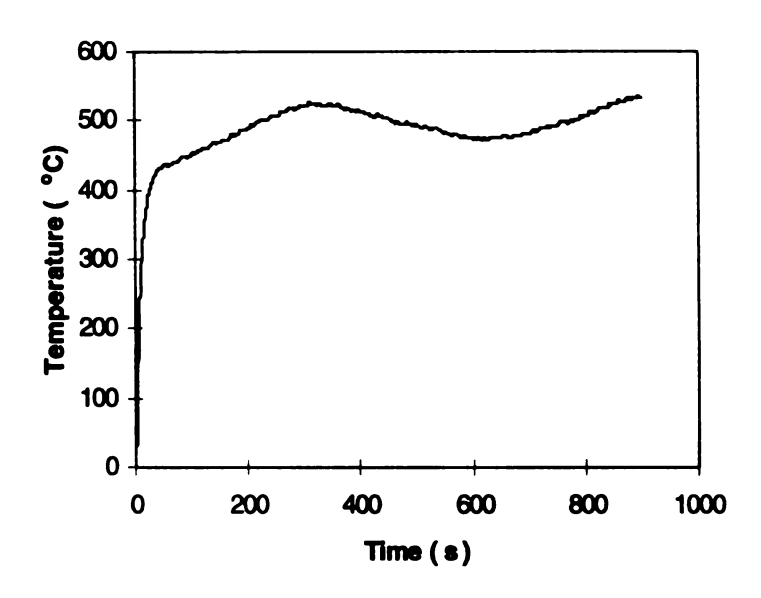


Figure 22. The temperature variation with 20 mm beam spot diameter, at 480 W power output, and a traverse speed of 0.105mm/s.

Although similar parameters have been tested in the previous section, such as small beam and fast traverse speed.

To determine what critical parameters for power output effectiveness are, the measurements were conducted by using two pairs of thermocouple connected to the two points, which are on a straight line. The thermocouples were separated from each other by 15 mm distance. Different beam transverse speed at 230 W power output were used, as shown in Figures 23, 24, and 25.

These graphs show that at certain power levels, the higher the scanning speed, the lower the peak temperature. The sharp peaks of the curves are clearly due to the high thermal conductivity of the aluminum alloy. The temperature difference between the two points can not be eliminated no matter how fast or how slow the beam traversed.

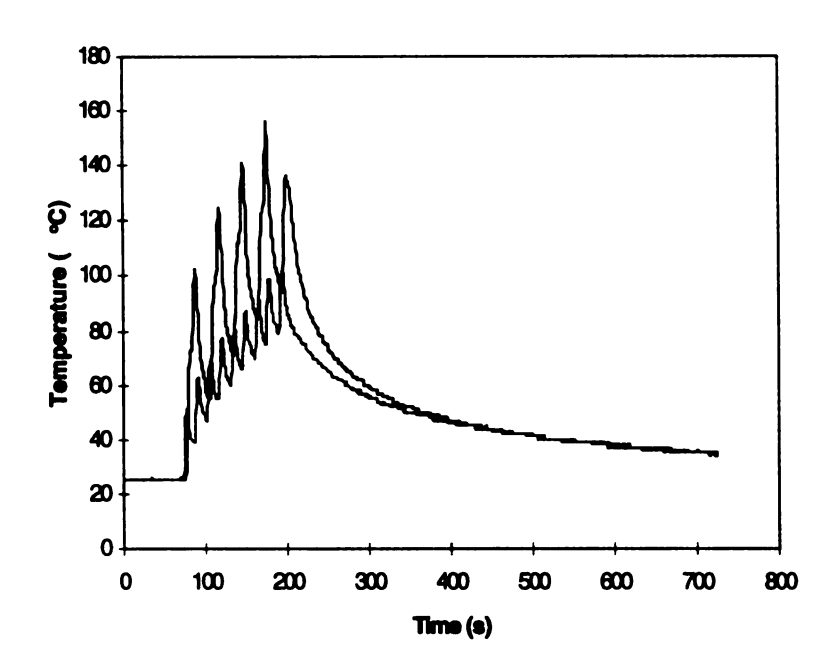


Figure 23. Two-point measurement. 230 W power output and 21.16 mm/s traverse speed at 5mm spot diameter.

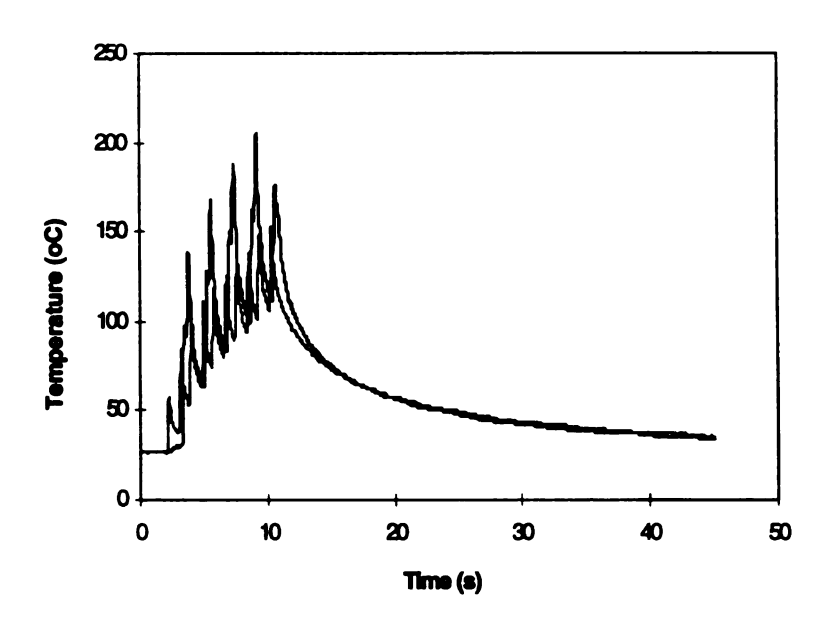


Figure 24. Two-point measurement. 230 W power output and 8.47 mm/s traverse speed at 5 mm spot diameter.

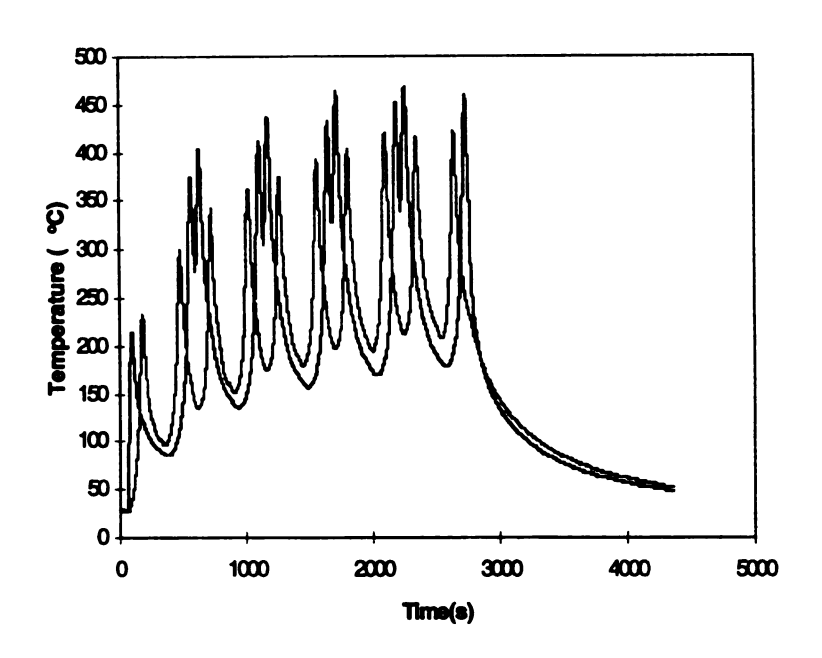


Figure 25. Two-point measurement. 230 W power output and 4.23 mm/s traverse speed at 5 mm spot diameter.

6.2.2 Center Point Measurement (static state)

Two-point temperature distribution curves have shown the influence of laser beam scanning speed, at a fixed beam size and power output. It could not be a good heating source for the conditions, taken such parameters as above, due to the unsteady temperature distribution. It has also been demonstrated in Figure 18, which shows the surface condition were treated improperly. However, what is the temperatures in the center of the workpiece, which can more truly reflect the heating conditions. For the center point measurement, a 20 mm diameter beam spot size was used, because in two-point measurements the small beam spot size could not work well.

By using larger beam spot size such as 20 mm, corresponding power output parameters were tested in the range of 345 to 370 watts, 470 to 490 watts, and at 570 watts. The corresponding temperature curves are shown in Figures 26, 27, and 28 respectively.

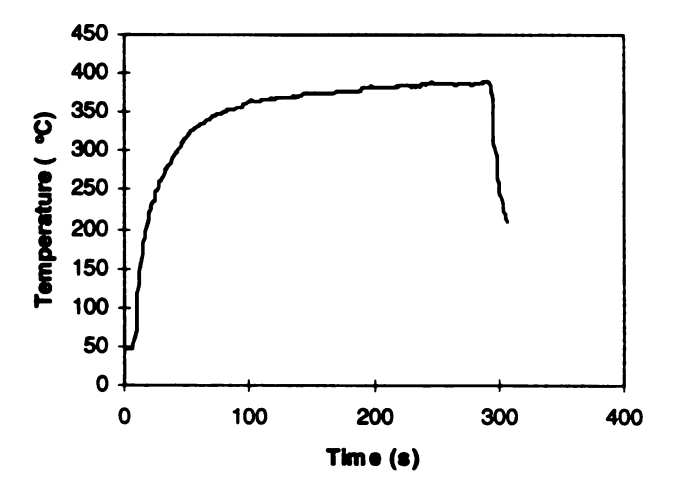


Figure 26. One point measurement. Power output 345 to 370 W spot diameter 20 mm at static state.

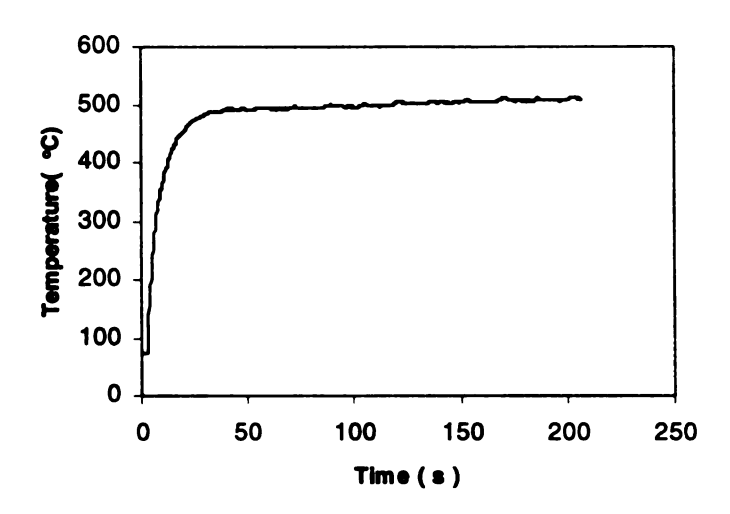


Figure 27. One point measurement. Power output 480 W, Spot diameter 20 mm at static state.

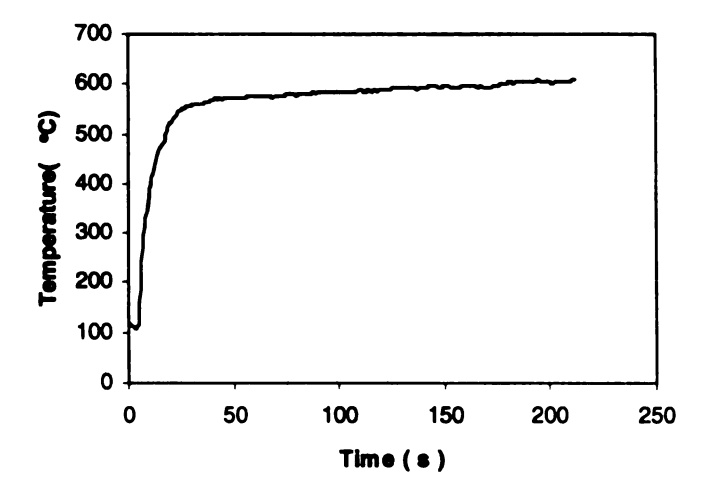


Figure 28. One point measurement. Power output 570 W, Spot diameter 20 mm at static state.

From the melting point of aluminum, the deformation temperature should be above 500 °C, since the superplastic deformed temperature is higher than about one half of the melting temperature in °K. Therefore, it is clear that when the power output was around 470 to 490 watts, the temperature of metal surface can reach up to 500 °C to 520 °C. Based on this distribution, an initial power output parameter was determined at around 470 to 500 watts, depending on the laser generator condition and ambient temperature situation.

6.2.3 Four Points Measurement (static state)

To get a reasonable temperature distribution at steady state, four thermocouples were connected on the bottom of the GK 45 aluminum alloy sheet at different points. They were located at (1) the center of the sample plate, (2) 13 mm off the center, it is a critical point since the largest beam spot diameter is 20 mm. This point was located approximately at the edge of the beam radiation zone, (3) 30 mm from the center, and (4) 50 mm from the center. The sketch of the temperature measurement has been shown in Figure 3, in Chapter 5. Four points were designed to be on a straight line. Figure 29 and Figure 30 show the curves of temperature vs time, tested at a laser power output of 490 W and 550 W, and the cover gas was 0.5 scfh (standard cubic feet per hour). The temperatures at different power setting are marked on the corresponding curves. From the temperatures shown in the Figure 24 and 25, it is seen that when laser power output was 490 W, the temperature at center point was about 528 °C. The temperature of the point that was 13mm off the center point was 405 °C. When laser power output was 550 W, the temperature of the center and 13mm off point were 590 °C and 445 °C

respectively. It is clear that within the region of laser beam diameter of 20 mm, the temperature zone can reach to 400 °C to 530 °C with 490 W power, and a temperature of 445 °C to 590 °C could be reached at 550 W. These figures also confirm that the thermal conductivity is very high, because the temperature difference between the center point and the point off 13 mm was about 125 °C at 490 W. When the power was 550 W, the temperature difference between these two points was 145 °C. These results indicate that the temperature of the point 13mm off the center can reach to the range of 450 °C to 500 °C.

Comparing the temperature measurement at the center point (from which an initial referenced parameters of laser power was considered as 470 W to 500 W), the results obtained from a four-point measurement indicated that the power output can be adjusted to around 500 W to 530 W, since the superplastic forming temperature for GK 45 aluminum alloy (AA 5083Zr) is about 500 °C to 550 °C.

The four-point temperature distributions (the time was chosen at 70 seconds) are shown in Figure 31 and 32.

Figures 31 and 32 indicate that the temperature at the center is the highest, despite the high thermal conductivity of aluminum. At the edge of the spot size, the temperature is within the superplastic deformation temperature, which has been discussed before, and it is a desired criterion. Another condition is that the amount of the cover gas flow also influences the temperature distribution. The degree of influence could be seen from the

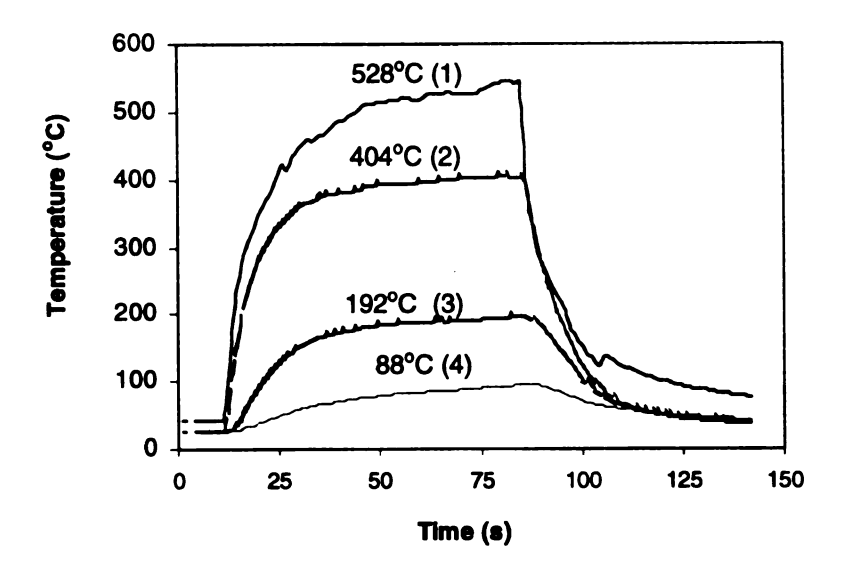


Figure 29. Four-point measurement. (1) center point of the plate, (2) 13 mm off the center, (3) 30 mm off the center, and (4) 50 mm off the center. Power output was 490 W.

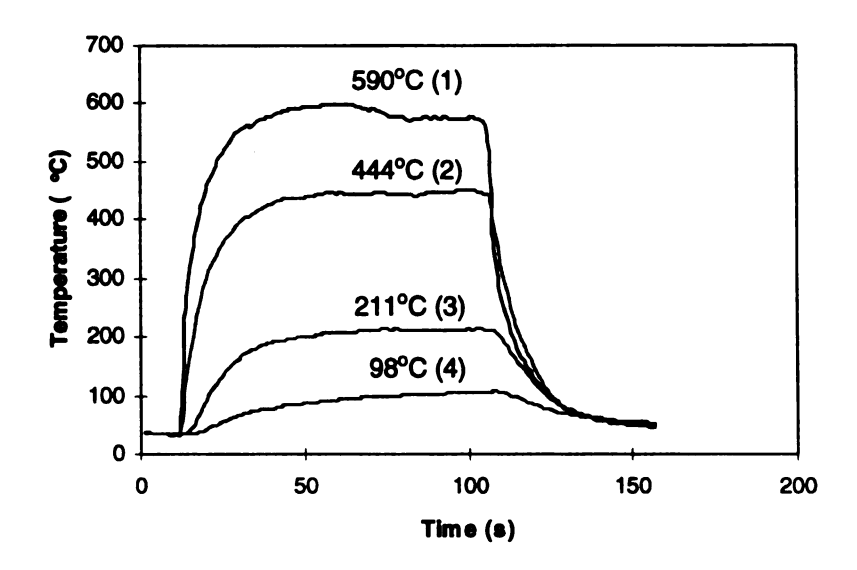


Figure 30. Four-point measurement. (1) center point of the plate, (2):13 mm off the center, (3) 30 mm off the center, and (4) 50 mm off the center. Power output was 550 W.

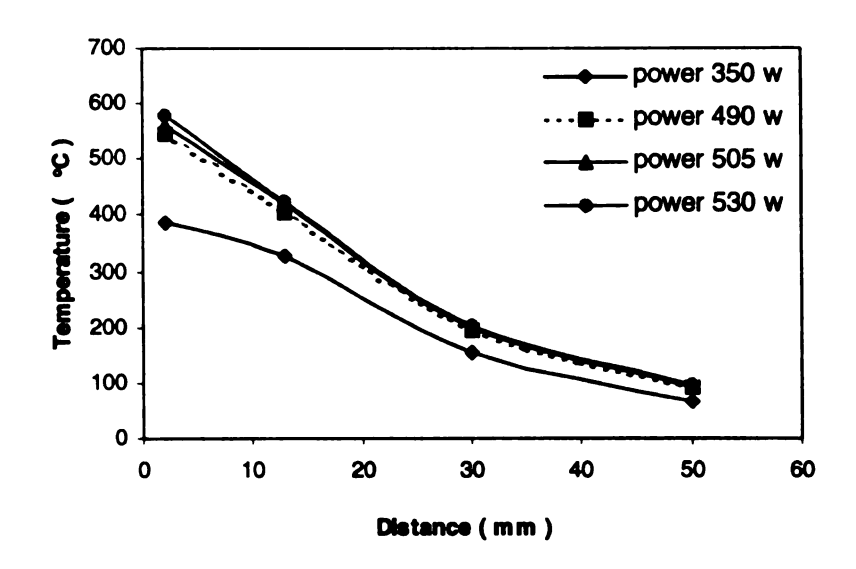


Figure 31. The temperature distribution at 70 seconds, 0.5 scfh cover gas

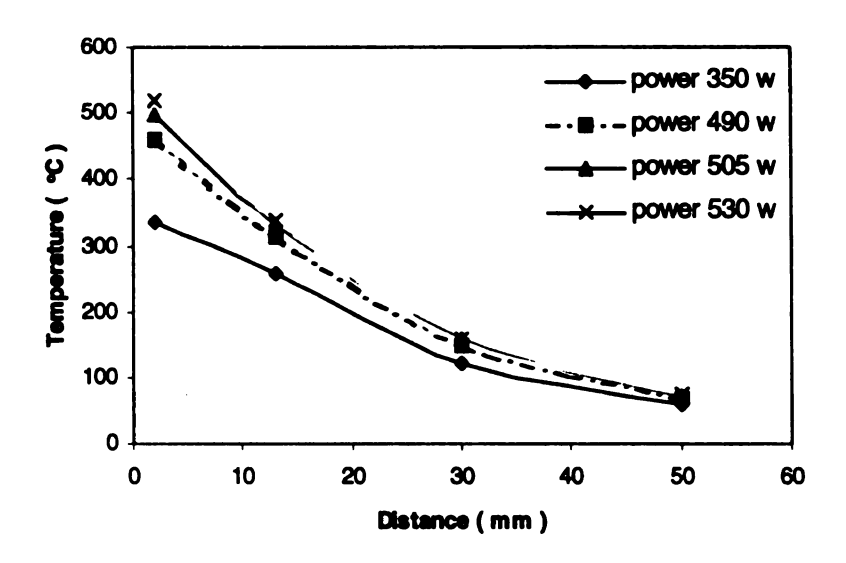


Figure 32. The temperature distribution at 70 seconds, 3.0 scfh cover gas

differences of the temperature profiles in Figure 31 and Figure 32. It is shown that the higher the cover gas flow, the more uniform the temperature distribution.

The time independent graphs are shown in Figures 33, 34 and 35. Every graph is plotted at certain power output conditions, and these graphs emphasize the temperature distribution at a steady state condition.

There are some common phenomenon in Figures 33, 34 and 35. First, the temperature distributions reach a steady state gradually after about 30 to 50 seconds. The highest temperature can be reached at 70 seconds, and the steady state is reached within a laser power of 350 W to 530 W. Secondly, the temperature gradient between the center point and fourth point, which is located at about 50 mm away from the center, is high when the beam power was on.

These graphs indicate that the thermal conductivity of the AA 5083Zr aluminum alloy is very high, which makes it difficult to establish a deforming temperature for localized superplastic forming. However, our results show that such a process is attainable.

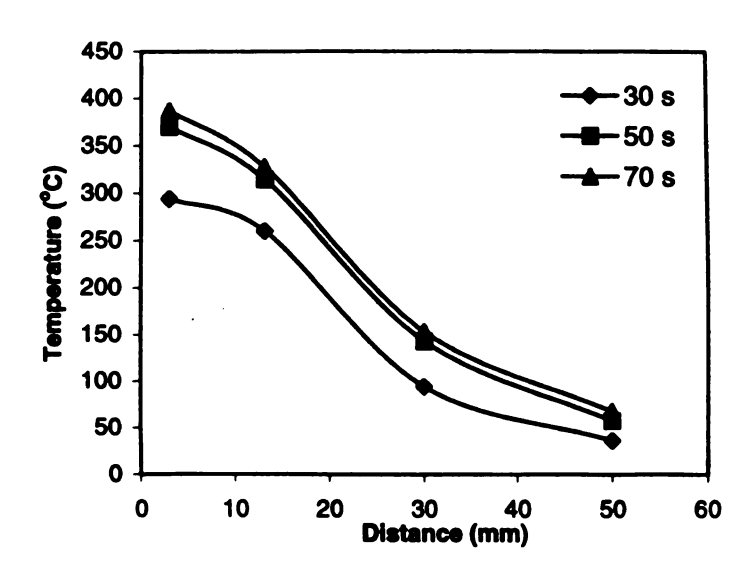


Figure 33. The temperature distribution at 350 W power output.

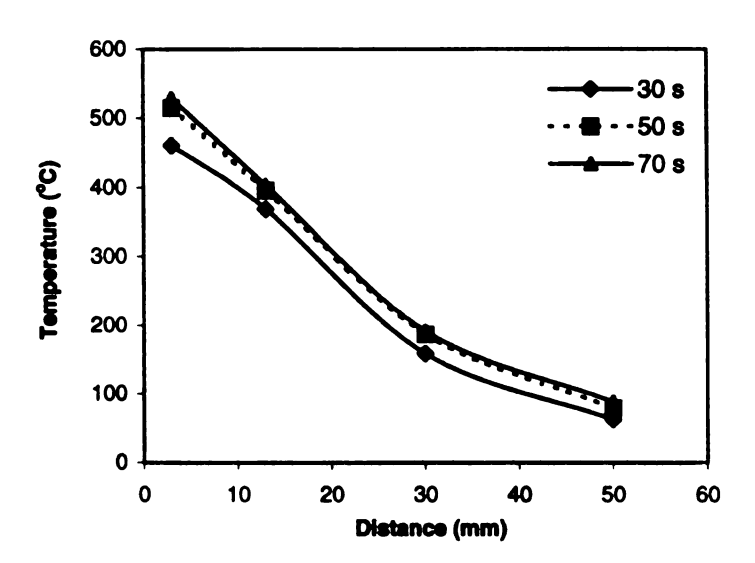


Figure 34. The temperature distribution at 490 W power output.

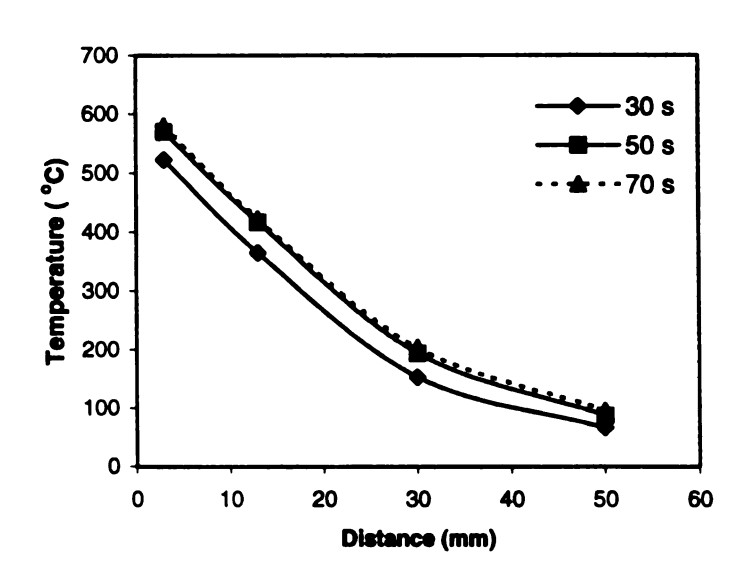


Figure 35. The temperature distribution at 530 W power output

6.3 Evaluation of Microstructure

It is well known that a fine and stable grain size can be maintained at high temperature is an essential requirement for superplastic deformation described as in Chapter 2. The superplastic potential of Aluminum alloys is critically dependent upon grain size stability, and cavitation.

6.3.1 Grain Growth at Furnace Heat Treatment

After getting a superplastically deformed sample, it is necessary to look at the grain growth tendency to see where or not the grain size remains in a condition for further superplastic deformation. Comparing the grain growth that occurred at the furnace heat treatment, and those occurred at laser aided deformation, it is concluded that the superplastic deformation is possible to produce actual parts.

First, some samples were treated in a furnace set at 450 °C, 500 °C, and 550 °C for 40 minutes. The laser heating time was usually longer because a loss of laser energy. Figures 36, 37 and 38 show the appearance of the microstructure for samples heated at 450 °C, 500 °C, and 550 °C for 40 minutes. The grain size was averaged from measurements taken in longitudinal and transverse directions. The corresponding grain sizes are 4.68 μm, 6.03 μm, and 8.08 μm respectively. The original grain size is about 5.48 μm, which is shown in Figure 39. From these results, it is seen that the temperature range, 450 °C to 550 °C, is proper for retaining the superplastic grain size. Many former researches have indicated that a grain size of approximately 5 to 10 μm is within the superplastic forming range. The grain growth tendency is plotted in Figure 40.

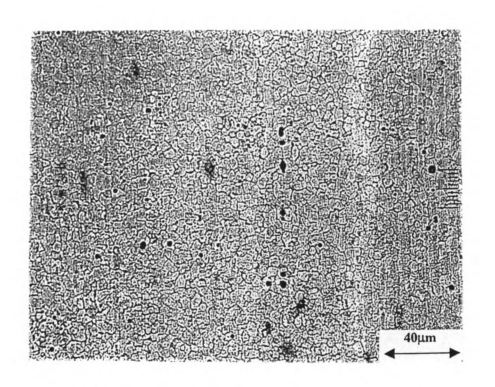


Figure 36. A photomicrograph showing the grain size after a 40 minute furnace annealing at $450^{\circ}C$

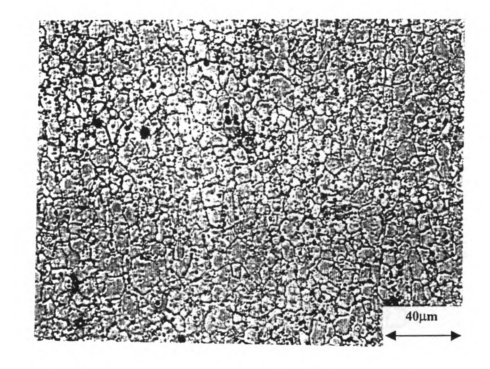


Figure 37. A photomicrograph showing the grain size after a 40 minute furnace annealing at 500° C

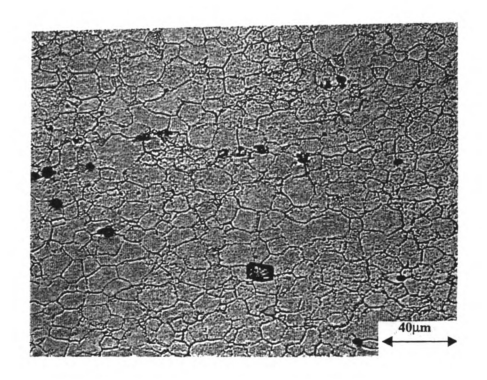


Figure 38. A photomicrograph showing the grain size after a 40 minute furnace annealing at 550°C .

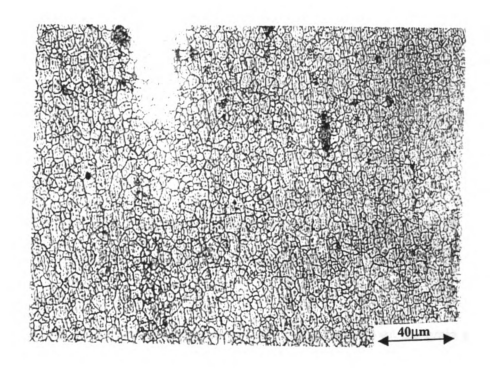


Figure 39. A photomicrograph showing the original grain size of GK 45 alloy

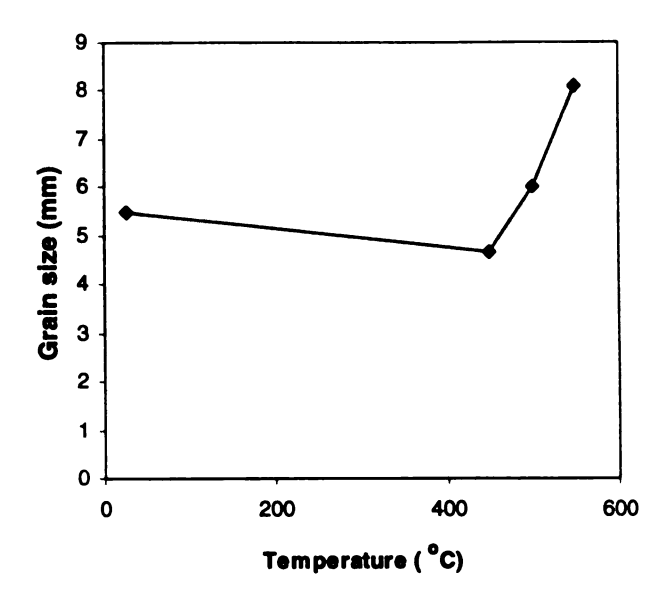


Figure 40. The curve showing the isothermal grain growth tendency at 40 minutes of furnace heating at temperature up to about 550 °C.

In above curve, the original grain size appears to be a little larger than the grain size after furnace heating up to about 500°C. The original sheet was in a cold rolled condition, and the grain shapes appear as elongated. After the temperature is raised, the microstructure apparently experience a recovery.

6.3.2 Grain Growth during Laser Process Heating

Figure 41 is a photograph showing the grain size at the bottom of the dome from a laser forming, which was processed at about 500°C, for a period of about 9.3 hours. The applied pressure difference was about 91.44 kPa (685.8 torr). The grain size is found to

be 8.81 µm. Comparing the grain growth data during furnace annealing, and during laser forming, it is found that the grain growth of GK 45 aluminum alloy during laser processing was a little faster than the grain growth at furnace anneal below 550°C.

6.4 Measurement of Strain and Strain Rate

The strain rate is an important indicator of the superplastic materials, and can be controlled by processing procedures. The profiles in Figure 42 were monitored by a surface profiler at every 20 minutes intervals during the processing. This set of deformation profile is shown at the progress of every 20 minutes, with three different power levels used. The length along the cross section of a sample versus time is plotted in Figure 43.

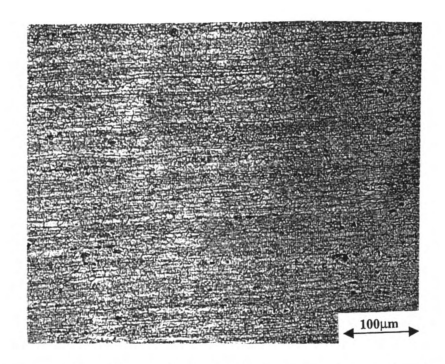


Figure 41. A photomicrograph showing the grain size at the bottom of a deformed dome in GK 45 sample

Deformation profiles at various stages

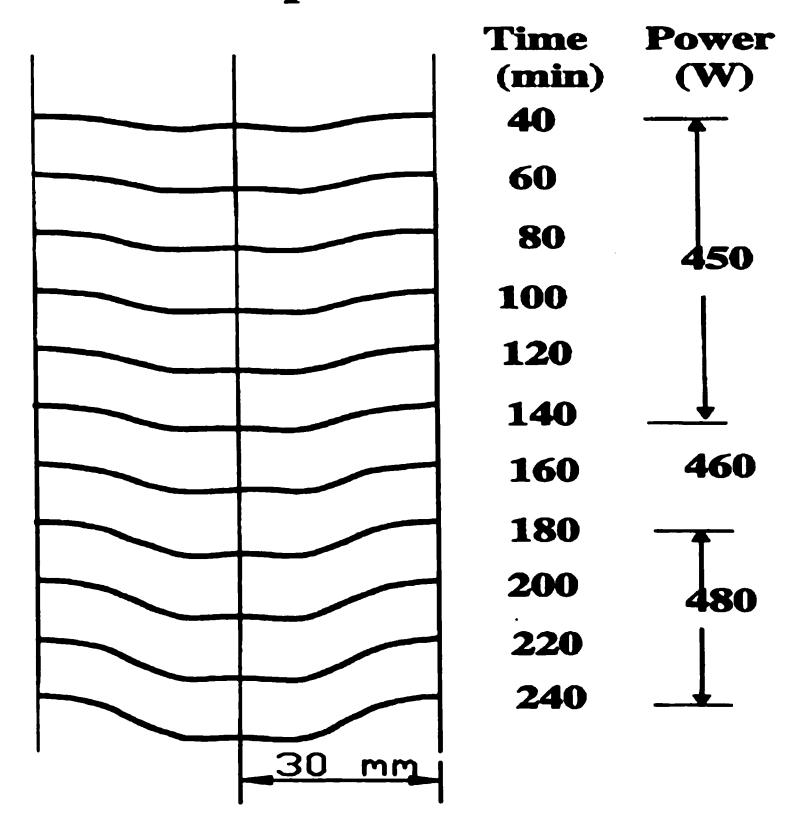


Figure 42. A set of deformation profiles, taken at 20 minutes interval during the processing

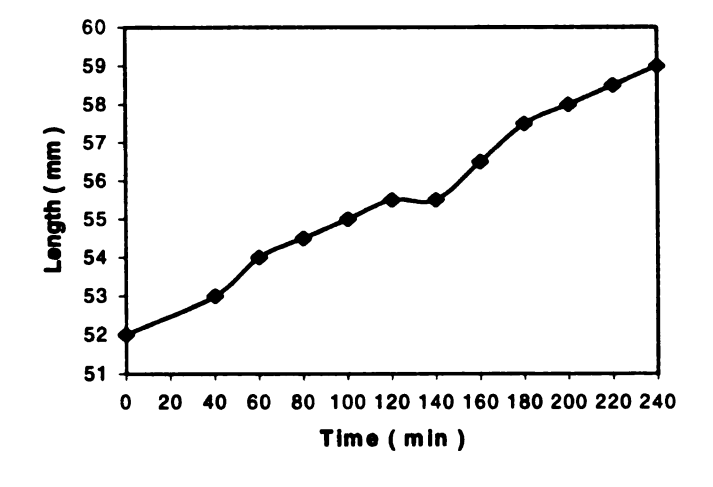


Figure 43. The length elongation of the cross section with process time.

The curve in Figure 43 demonstrates that the deforming progress was regularly 1 mm at the beginning, and gradually decreased with the increasing time. Beyond the running time of 120 minutes, there was no length difference for another 20 minutes of processing.

After increasing the power from 450 W to 460 W, the increment was made noticeable again. At 480 W, the slope of the curve becomes gentle. For example, the variation of the sample length from 0.5 mm to 1.0 mm occurs after increasing the power output. Thus, these two cycles indicate that GK 45 has the potential to continue the superplastic deformation if the energy is increased.

The strain and strain rate were calculated by measuring the variation of the thickness.

The idea of calculation for strain and strain rate by the thickness variance is that the volume of the superplastically deformed region is unchanged. Suppose that T_o is the original thickness, and T is the final average thickness of the deformed sample. According to the principle of the volume conservation, the original volume S_oT_o should be equal to the final volume ST, that is

$$S_0 T_0 = ST, (6-4)$$

Therefore, from equation (6-4), we can write the following expression as below:

$$(To - T)/T = (S - So)/So$$
 (6-5)

Where S_o is the original deformation area and S is the final average area.

The strain ε , is expressed by

$$\varepsilon = (L-Lo)/Lo \tag{6-6}$$

Under the plastic flow condition, the volume is equal to each other between deformed and undeformed specimen. Thus,

$$LoAo = LA (6-7)$$

Where Lo is original length of the original sample and L is final length of the sample.

Ao is the area of the original cross section, and A represents the area of the deformed cross section. From equation (6-7), a similar expression to equation (6-5) follows:

$$(Lo - L)/L = (A - Ao)/Ao$$
 (6-8)

Comparing equation (6-5) and (6-8), and from the concept of Equation (6-6), the conclusion is that:

$$(T - To)/To = \varepsilon$$

So the strain ε can be calculated through the formula of thickness variance $(T - T_0)/T_0$. By this way, it simplified the problem of strain measurement in a large scale.

Figures 44 and 45 are the sketches of the cross section of the deformed samples with different forming stresses. The sketch of the cross section shown in Figure 42, was taken from the sample which deformed at 91.44 kPa (685.8 torr) applied pressure and the total forming time was 240 minutes. Figure 43 shows the appearance of the cross section from a sample, which deformed at 200 kPa (2 bar) argon gas and the processing period was around 110 minutes. The thickness variance along the cross section is marked on the corresponding locations individually.

In Figure 44, the data of the original thickness of the sample, To is equal to 1.6612 mm (0.0654 inch), and the final thickness of the cross section of the deformed sample is averaged as T is equal to 1.3665 mm (0.0538 inch). Since $\varepsilon = [(T - T_0)/T_0] \times 100\%$,

the computed strain ε is equal to 17.74 %. The strain rate corresponding to 240 minutes is,

$$\epsilon$$
 = 1.23 x 10⁻⁵ s⁻¹

The thickness variation shown in Figure 45 were measured from the original thickness. Since To is equal to 1.6612 mm (0.0654 inch), and the average final thickness T is equal to 1.3183 mm (0.0519 inch), The stain ε is about 20.64 % and the relevant stain rate for 110 minutes is,

$$\epsilon$$
 = 3.13 x 10⁻⁵ s⁻¹

From the values of the stain rate for the above two samples, it is obvious that when the applied stress increased, the strain rate increased also. Thus, the strain rate was not only controlled by temperature but also by the forming stress applied on the deformed region. Thus, for GK 45 alloy, there is a potential to increase the deformation speed as well.

6. 5 The Variation of Thickness

A perfect superplastic deformation should have a uniform thickness at any region of the final shape. However, that is very difficult to achieve. Usually, the corners have the thinnest gage section in conventional superplastic forming. Thus, the stress, distribution on the deformed region would become increasingly non-uniform.

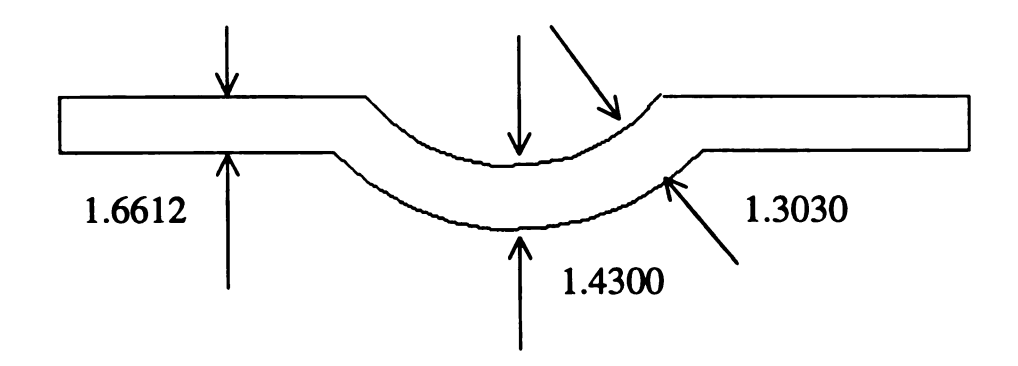


Figure 44. A sketch of the cross section showing the thickness variance with vacuum forming system.

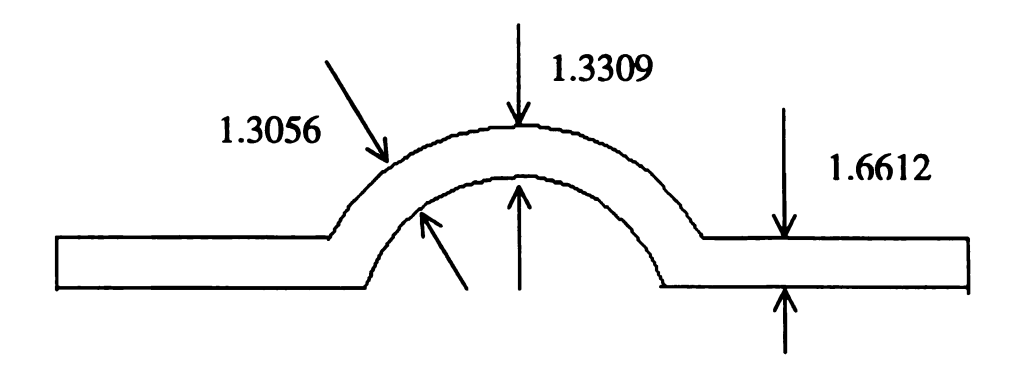


Figure 45. A sketch of the cross section showing the thickness variance with argon gas forming system.

Figures 46 and 47 are photographs showing the cross section of the sample which were processed separately in vacuum forming system, and in argon gas forming systems. The processing time and applied stress, as well as the corresponding strain rate have been discussed in Section 6.3. The deformations were achieved in the following schematic processing picture as showing in Figure 48. The scanning patterns were processed by scanning around a circle, and then a stationary laser beam was used on the center of pattern.

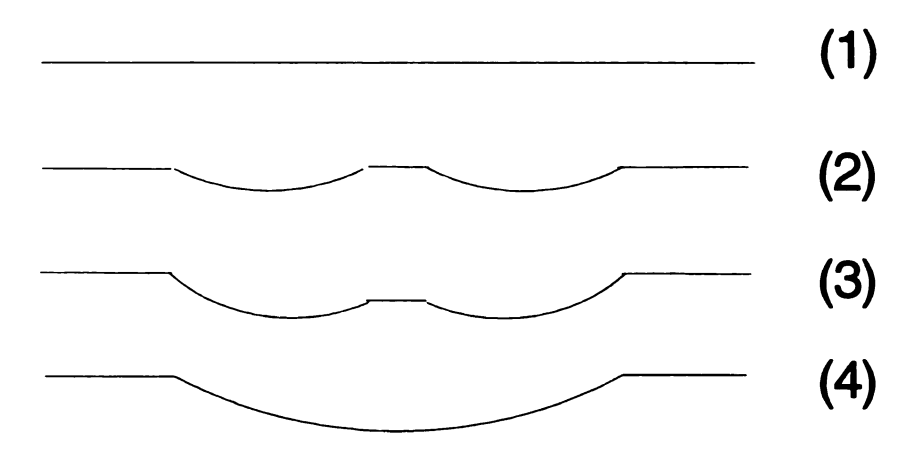


Figure 48. A schematic sketch of showing the deformation process by a laser beam scanning around a circle, and a stable irradiation at the center.

Initial stage is shown in (1), and the final stage is shown in (4).

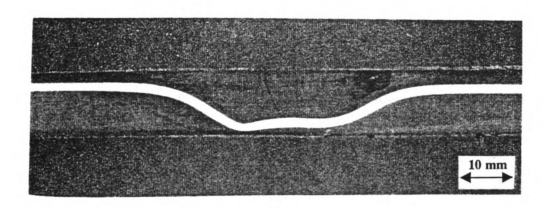


Figure 46. A photograph showing a cross-section appearance of a sample deformed by introducing vacuum.

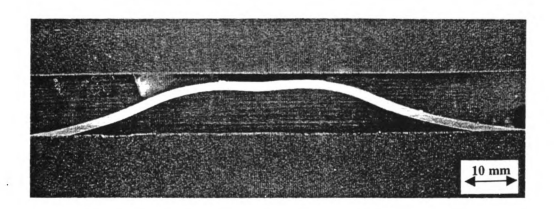


Figure 47. A photograph showing a cross-section appearance of a sample deformed by argon gas.

The thickness variation shown in Figure 45 looks more uniform than that shown in Figure 46. Note that argon gas can applied higher stress than vacuum system, therefore the deformation rate was higher than the former.

The factors that contribute to the thinning characteristics are complex. For example, thickness variations or materials inhomogeneities will cause local stress differences leading to localized thinning.

The applied pressure and stress distribution, temperature distribution and laser beam scanning patterns are dominant parameters to laser assisted superplastic forming processing. This study has been the very first such results accomplished through laser forming. Figure 49 is a photograph of such a dome produced with GK 45 alloy by laser assisted superplastic forming as developed in this thesis.

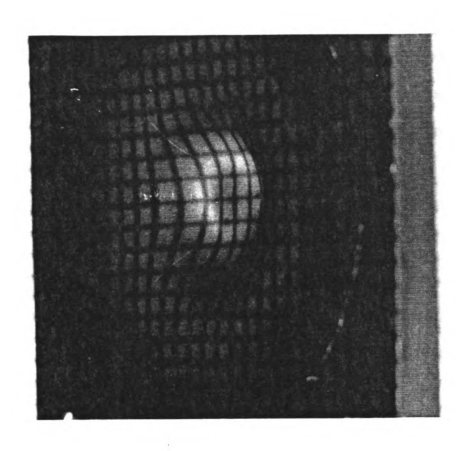


Figure 49. A photograph of a dome produced by LSF in GK 45 alloy. A square-mesh grid pattern is projected on the sample to help visualize the curvature.

Chapter 7

SUMMARIES

The following summaries can be derived from the experimental results.

- The feasibility of laser, dieless superplastic forming of materials have been demonstrated from this research. This technique involves a high energy CO₂ laser beam as the dynamic heat source and a computer numerical by controlled motion system. The laser beam scanning pattern can be programmed via CNC code, and performed by a x-y moving table. A desired deformation shape could be obtained by programming the beam heating geometry, and controlling the heat input through laser.
- From the investigation of microstructure of GK45 aluminum alloy, the superplastic deformation temperature is around 500°C to 550°C, the corresponding laser power output needed is around 460 W to 490 W, depending on the ambient temperature, and the temperature of the cooling water.
- In order to obtain effective deformation, the influence of high thermal conductivity of the alloy must be considered. For a laser beam diameter of 20 mm, a relative slow laser beam traverse speed around 0.10 to 0.20 mm/s were found to be the best choice.
- Since cold-rolled aluminum sheet exhibits shining surface, it has very low absorption
 of laser energy. To enhance absorption of infrared CO₂ laser, the sheet metal has to
 be prepared by reagent etching, high temperature painting, and subsequently baking
 at 200 °C.

- From the measurement of strain and calculation of the strain rate, a deformation saturation is absorbed, although the deforming limit was not achieved.
- The final thickness variance, measured from the cross section, is not very uniform.

 However, it could be improved by controlling the laser heating path or by providing higher pressure for speeding deformation rate, and therefore to increase strain rate.

BIBLOGRAPHY

- 1. K.A.Padmanabhan, G.J.Davies "Superplasticity Mechanical and Structural Aspects, Environmental Effects, Fundamentals and Applications "Springer-Verlag 1980.
- 2. Oleg D. sherby and Jeffrey Wadsworth: Superplasticicty Recent Advances and FurureDirections. *Matrials Science* Vol. 33, pp. 169-221, 1989
- 3. Amiya K. Mukherjee: Superplastic in Metals, Ceramics and Intermetallics *Plastic Deformation and fracture of materials* Vol. 6 chap. 9
- 4. John I. Duncan, stuart P. keeler, Harmon D. Nine and Philip A. Stine: Sheet Metal Formability. *Tool and Manufacturing Engineers Handbook* Vol.2 pp. 1-20, 1983
- 5. C.H. Hamilton: Superplastic sheet Forming. *Metals Handbook Ninth Edition*. Vol. 14 pp.852, 1988
- 6. Sokka M. Doraivelu, Lowell W. Foster, Harold L. Gegel: Superplastic Forming.

 Tool and Manufacturing Engineers Handbook Vol.2 pp. 4-59, 1983
- 7. M.M. I. Ahmed and T.G.Langdon, Metall. Trans 8A, pp.1832. 1977
- 8. Y.Nakatani, T. Ohnishi and K. Higashi, J. Japan Inst. Metals 48, pp.113. 1984
- 9. K. Higashi, T. Ohnishi and Y. Nakatani. Scr. Metall. 19, pp.821. 1985
- 10. T. G. Langdon, Private Communication, on the work Y. Ma and T. G. Langdon, University of Southern California. 1988
- 11. K. Higashi, Private Communication. 1988
- 12. J. W. Edington, K. N. Melton and C.P.Cutler, Prog. Mater. Sci. 21(2), 61 1976
- 13. O. D. Sherby and J. Wadsworth, American Society for Metals Park *Deformation*, *Progressing and Structure*. pp. 355. 1984
- 14. O. D. Sherby and J. Wadsworth, Mater. Sci. and Tech 1,925. 1985.
- 15. W. A. Backofen, I. R. Turner and D. H. Avery, *Trans. Am. Soc. Metals* 57, 980 1964.
- 16. N. E. Paton and C.H. Hamilton, The Metallurgical Society of AIME. Warrendale, PA 1982 Superplastic Forming of Structural Alloys.

- 17. C. H. Hamilton: Superplastic Forming of Aluminum. *International Show of Technologies and Energies of the Future*. Toulouse, France, 1981
- 18. Nicholson, R.B.: Electron Microscopy and the structure of materials. Berkeley, University of California. pp.689. 1972
- 19. Baudelet, B.; Suery, M.: Mater. Sci. vol 7 pp.512. 1972
- 20. Avery, D. H.; Backfen. W.A.: Trans. Am. Soc. Met. Vol. 58 pp.551 1965
- 21. Holt, D.L.; Backfen, W.A.: Trans. Am. Soc. Met. Vol. 59 pp.755. 1966
- 22. Cline, H.E.; Alden, T.H.: Trans. Met. Soc. AIME Vol. 239 pp.710 1967
- 23. Zehr, S. W.; Backfen. W.A.: Trans. Am. Soc. Met. Vol. 61 pp.300. 1968
- 24. Lee, D.: Acta Metall. Vol. 17 pp.1057. 1969
- 25. Sagat, S.; Blenkinsop, P.A.; Taplin, D.M.R.: J. Inst. Met. Vol.100 pp.268. 1972
- 26. Marder, A.R.: Trans. Met. Soc. AIME Vol. 245 pp.1337 1969
- 27. Horiuchi, R., El-Sebai, A. B.; Otsuka, M.: Scripta Metall Vol.7 pp.1101. 1973
- 28. Stewart, M. J.: *Metall. Trans.* Vol. 7A pp.399. 1976
- 29. Garde, A.M., Chung, H.M., Kaussner, T.F.: Acta Metall. Vol. 26. pp. 153 1978
- 30. J. A. Wert, N.E. paton, C. H. Hamilton and M. W. Mahoney: Metall. Trans. A, Vol.12A, pp.1265. 1981
- 31. B.M. Watts, M.J. Stowell, B. L. Baikie and D.G.E. Owen: Met. Sci. Vol 10, pp.198 1976
- 32. D. C. Winburn, What Every Engineer Should Know About LASERS. New York and Basel. 1987
- 33. J. F. Ready, Industrial Applications of Lasers. New York, Academic Press, 1978
- 34. J.E. Harry, Industrial Lasers and Their Applications. New York, McGraw-Hill, 1974.
- 35. Hans Koebner, *Industrial Applications of Lasers*. Chichester, New York. A Wiley-Interscience. 1984.

- 36. R. C. Crafer and P. J. Oakley, "Process and physical aspects of continuos wave laser processing "in Applied Laser Tooling, pp. 55 79, Martinus Nijhoff Publishers, 1987.
- 37. Y. Arata and I. Miyamoto, "Some fundamental properties of high power laser beam as a heat source, "in Plasma, Electron & Laser Beam Technology (Y. Arata, Ed.), pp.233-262, ASM, Metals Park, OH, 1986.
- 38. K. Mukherjee, C. W. Chen and N. Hu, "Laser Dieless Forming of Plastic and Superplastic Materials" in TMS conference, Cincinnati, 1996.
- 39. J. M. Poate, G. Foti, and D. C. Jacobson. Surface Modification and Alloying by Laser, Ion, and Electron Beams. New York and London Plenum Press, 1983.
- 40. S. S. Charschan and R. Webb, "considerations for lasers in manufacturing, "in Laser Materials Processing (M. Bass, Ed.) ch. 9, pp439-473, North-Holland Pub. Co., 1983.
- 41. G. Chryssolouris, Laser Machining: Theory and Practice. New York: Springer-Verlag, 1991.
- 42. Clifton W. Draper and Paolo Mazzoldi, Laser Surface Treatment of Metals. Martinus Nijhoff Publishers, 1986.
- 43. T. Lehecka, N. C. Luhmann, Jr., W.A. Peebles, J. Goldhar, and S.P. Obenschain, "Gas Lasers," in *Handbook of Microwave and Optical Components* Vol. 3, pp. 451-596, John Wiley & Sons, 1990.
- 44. B.A. Lengyel, *lasers*. New York: Wiley-Interscience, 2ed., 1971.
- 45. J. T. Luxon, D. E. Parker, and P.D. Plotkowski, *Lasers in Manufacturing*. New York: IFS (Pub.) Ltd. And Springer-Verlag, 1987.
- 46. W. W. Duley, CO₂ Lasers Effects and Applications. New York: Academic Press, 1976.
- 47. D. C. O'Shea, W. R. Callen, and W. T. Rhodes, *Introduction to lasers and Their Applications*. Reading, MA: Addison-Wesley, 1977.
- 48. B. A. Lenyel, Introduction to Laser Physics. New York: John Wiley & Sons, 1967.
- 49. K. Mukherjee and J. Mazumder, Laser Processing of Materials. Warrendale, PA: AIME Publication, 1985.

- 50. J. Mazumder and K. Mukherjee, Laser Materials Processing III. Warrendale, PA: TMS Publication, 1989.
- 51. J. Mazumder and K. Mukherjee, and B. L. Mordike, Laser Materials Processing IV. Warrendale, PA: TMS Publication, 1994.
- 52. R. Migliroe, "Laser cutting," in *Engineered Materials Handbook*, Composites, vol.1, pp. 676-680, ASM International, 1988.
- 53. R. R. Schrelber, "Lasers: Technology advances are boosting the usefulness of CO2, Nd: YAG, and excimer lasers in manufacturing. Part I, "Manufacturing Engineering, vol. 106, pp.41-44, January 1991.
- 54. R. R. Schrelber, "Lasers: Lasers can help you cut up the competition. Part II, " *Manufacturing Engineering*, vol. 106, pp. 281-290, Febrary 1991.
- 55. P. W. Milonni and J. H. Eberly, Lasers. New York: John Wiley & Sons, 1988.
- 56. I. Miyamoto, T.Ooie, Y.Hirota, and H. Maruo, "Mechanism of laser ablation Ablation process and debris formation, "in *Laser Materials Processing*, vol. SPIE 2306, pp. 1-11, Laser Institute of America, 1993.
- 57. E. M. Breinan and B. H. Kear, "Rapid solidification laser processing at high power density, "in *Laser Materials Processing* (M. Bass, Ed.) ch 5, pp.234-295, North-Holland Pub. Co., 1983
- 58. Z. Sun and J. C. Ion, "Review: Laser welding of dissimilar metal combinations, "J. *Materials Science*, vol.30, no.17, pp.4205-4214, 1995.
- 59. A. V.L. Rocca, "Laser applications in manufacturing, "Scientific American, vol. 246, no.3, pp.94-103, 1982.
- 60. S. Saending and P. Wiesner, "Laser surface melting of cutting tool materials," in Laser Materials Processing vol.2306, pp.835-846. 1994.
- 61. R. Vilar, R. Colaco, and A. Almerda, "Laser surface treatment of tool steels," *Optical and Quantum Electronics*, vol. 27, no.12, pp.1273-1289, 1995.
- 62. C. Marsden, D.R.F. West and W. M. Steen, "Laser Surface Alloying of Stainless Stell with Carbon," in *Laser Surface Treatment of Metals*, pp. 461-474. 1986.
- 63. E. Gaffet, J. M. Pelletier, and S. Bonnet-Jobez, "Laser surface alloying of Ni film on Al-based alloy," *Acta Metallurgica*, vol.37, no.12, pp. 3205-3215, 1989.

- 64. A. Almeida, R. Vilar, and R. Colaco, "Laser alloying of Al and 7175 Al alloy for Enhanced corrosion resistance, "in *Laser Materials Processing*, vol. 2306, pp. 903-912, 1994.
- 65. S. Yerramareddy and S. Bahadur, "Effect of laser surface treatments on the tribological behavior of Ti-6Al-4V," Wear, vol. 157. No.2, pp. 245-262, 1992.
- 66. O. V. Akgun and O. T. Inal, "Laser surface modification of Ti-6Al-4V alloy," in *Journal of materials Science*, vol. 29, no.5, pp.1159-1168, 1994.
- 67. I. C. Hawkes, A. M. walker, "Applicattion of laser surface melting and alloying to alloys based on the FE-C system," in *Laser Processing of Materials* pp. 169-182 1985.
- 68. M. Pridham and G. Thomson, "Laser forming: A force for the future?" Materials World. Nov. 1994.
- 69. M. Geiger, "Synergy of Laser Material Processing and Metal Forming" CIRP annalsmanufacturing technology. Vol. 43, no.2 pp.563-569. 1994.
- 70. Geifer, M.; Vollertsen, F.; Deinzer, G., "Flexible Straightening of Car Body Shells by Laser Forming." S.A.E. transactions. Vol.102, no.5 pp.354-361. 1994.
- 71. Vollertsen, F., "Potentials of laser forming" in *Laser und optoelektronik*. Vol 27, no.3 1995.
- 72. Nakagawa, T; Makinouchi, A; Wei, J; Shimizu, T., "Application of laser stereolithography in FE sheet- metal forming simulation." *Journal of materials processing technology*. Vol 50, no. 1-4. 1995.
- 73. Vaccari, John A. "The promise of laser forming" *American machinist*. Vol.137, no.6. 1993.
- 74. Veiko, V. P.; Yakovlev, Y. B. "Physical fundamentals of laser forming of micro-optical components." Optical Engineering: vol.33, no 11. 1994.
- 75. O. D. Serby and J. Wardswoth, "superpalsticity Recent Advances and Future directions," in Material Science. vol.33, pp.169, 1989.
- 76. P. J. Winkler, "Superplasticity in Use: A Critical Review of its Status, Trends, and Limits", MRS symposium Proc., vol. 196, 1990.
- 77. N. Dahotre, Anne Hunter, and K. Mukherjee, "Laser Hardening of W2 tool steel," in J. Mat. Science, vol 22, 403 1987.

- 78. S. Kudapa, V. Barnekov and K. Mukherjee, "Laser Machining and Joining of Composites" in Laser Materials Processing IV, TMS Publication, pp.223 1987.
- 79. Yiping Hu, "Laser cladding of hard-facing Materials onto AISI 1045 Steel for Patterned Cutting-Die Design" Thesis, 1996.

